

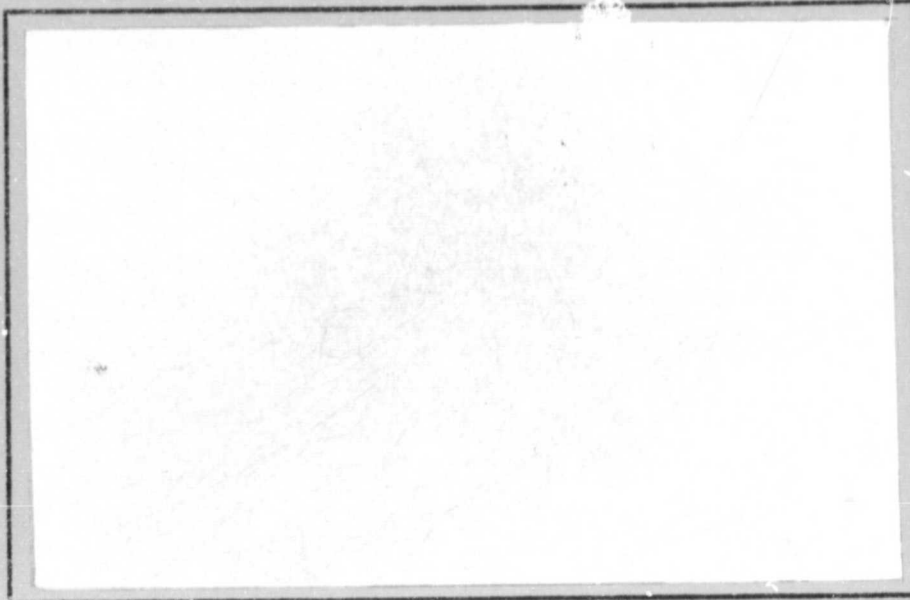
N O T I C E

THIS DOCUMENT HAS BEEN REPRODUCED FROM
MICROFICHE. ALTHOUGH IT IS RECOGNIZED THAT
CERTAIN PORTIONS ARE ILLEGIBLE, IT IS BEING RELEASED
IN THE INTEREST OF MAKING AVAILABLE AS MUCH
INFORMATION AS POSSIBLE

(NASA-CR-162903) A FUNDAMENTAL APPROACH TO
ADHESION: SYNTHESIS, SURFACE ANALYSIS,
THERMODYNAMICS AND MECHANICS Final Report
(Virginia Polytechnic Inst. and State Univ.)
128 p HC A07/MF A01

N80-20397

Unclassified
CSCL 11A G3/27 46740



**Virginia Polytechnic Institute
and State University**

Chemistry Department

Blacksburg, Virginia 24061



FINAL REPORT

A FUNDAMENTAL APPROACH TO ADHESION:
SYNTHESIS, SURFACE ANALYSIS,
THERMODYNAMICS AND MECHANICS

by

Ranjani Siriwardane and James P. Wightman

Prepared for

National Aeronautics and Space Administration

March, 1980

Grant NSG-1124

NASA-Langley Research Center
Hampton, Virginia 23665
Materials Division
Donald J. Progar

Department of Chemistry
Virginia Polytechnic Institute and State University
Blacksburg, Virginia 24061

FOREWARD

The major portion of this year's effort at Virginia Polytechnic Institute and State University was concerned with the spectroscopic characterization of the surface acidity of titanium 6-4 adherend surfaces. This work is described starting on p. iv.

A second major thrust of this grant is polymer synthesis carried out by Paul M. Hergenrother, Adjunct Research Professor, at NASA-LaRC. A summary of this work on polymer synthesis is given in Appendix II.

PRECEDING PAGE BLANK NOT FILMED

TABLE OF CONTENTS

	<u>page</u>
FOREWARD	iii
LIST OF TABLES	vii
LIST OF FIGURES	x
<u>CHAPTER</u>	
I INTRODUCTION	1
II LITERATURE SURVEY	3
(A) Acid-Base Theories	3
(B) Indictor Theories and Indicator Method	5
(C) Acid Strength and Hammett Acidity Functions	8
(D) Other Methods Used in the Determination of Acid-Base Properties of Surfaces	14
1. Aqueous methods	14
2. Non aqueous liquid phase methods	16
3. Adsorption from gas phase	19
4. Hydrogen-deuterium exchange reactions	20
5. Optical spectroscopy	20
(E) Characterization Techniques	22
III EXPERIMENTAL	25
(A) Materials	25
1. Indicators	25
2. Solvents	25
3. Solid materials	31
4. Materials used in the pretreatment	31
5. Adsorbates	31
(B) Visual Color Changes of the Indicators on Powders	31
(C) Determination of Maximum Wavelength of Absorption of the Indicators	31

	<u>Page</u>
(D) Preparation of Titanium 6-4 Metal Coupons and Indicator Solutions	32
(E) Visible Diffuse Reflectance Spectroscopy	33
(F) Variations of the Experimental Conditions	35
1. Effect of drying time	35
2. Effect of solvent	35
3. Effect of concentration of the indicator solutions	35
4. Effect of temperature	36
5. Effect of relative humidity	36
6. Effect of drying environment	36
(G) ESCA Measurements	37
(H) Stearic Acid Adsorption	39
(I) Specular Reflectance Infra-Red Spectra	39
IV. RESULTS AND DISCUSSION	41
PART I: Study of Solid Powders	41
PART II: Study of Titanium 6-4 Metal Coupons with Indicators	45
(A) The Visible Absorption Spectra of the Indicators	45
(B) Surface Pretreatments	45
(C) Effect of Experimental Conditions	56
1. Time effects	56
2. Effect of solvent	61
3. Effect of concentration of the indicators ...	61
4. Temperature effects	65
5. Relative humidity effects	71
6. Effect of drying conditions	71
PART III: Electron Spectroscopy for Chemical Analysis	76
(A) Bare Ti 6-4 Metal Coupons after Pretreatments	76

	<u>Page</u>
(B) Bromthymol Blue Indicator Spread on the Pretreated Ti 6-4 Metal Coupons	81
(C) Pretreated Metal Coupons Immersed in the Brom- thymol Blue Solution	86
(D) Pretreated Metal Coupons Immersed in the Thymol Blue Solution	86
PART IV: Specular Reflectance Infra-Red Spectra	90
PART V: Model for Ti 6-4 Surface	98
V. CONCLUSIONS	106
REFERENCES	108
APPENDIX I	112
APPENDIX II	115

LIST OF TABLES

<u>TABLE</u>		<u>Page</u>
I	COLORS OF THE INDICATORS ADSORBED ON VARIOUS SOLIDS (10)	9
II	ACID STRENGTH OF SOME SOLIDS (4)	13
III	INDICATORS USED IN THE STUDY OF SOLID POWDERS	26
IV	INDICATORS USED IN THE STUDY OF Ti 6-4 METAL COUPONS ..	28
V	SOLUBILITIES OF INDICATORS IN VARIOUS SOLVENTS	42
VI	COLOR CHANGES OF THE INDICATORS ON SOLID POWDERS	43
VII	COLORS AND λ_{MAX} VALUES OF THE ACID AND BASE FORMS OF THE INDICATORS	46
VIII	λ_{MAX} VALUES AND COLOR CHANGES OF THE INDICATORS ON TURCO ETCHED TITANIUM 6-4 SURFACE	51
IX	λ_{MAX} VALUES AND COLOR CHANGES OF THE INDICATORS ON PHOSPHATE-FLUORIDE ETCHED Ti 6-4 SURFACE	52
X	λ_{MAX} VALUES AND COLOR CHANGES OF THE INDICATORS ON PASA-JELL ETCHED Ti 6-4 SURFACE	53
XI	TIME EFFECTS ON PHOSPHATE-FLUORIDE ETCHED Ti 6-4 SURFACE WITH BROMTHYMOL BLUE	57
XII	TIME EFFECTS ON PHOSPHATE-FLUORIDE ETCHED Ti 6-4 SURFACE WITH THYMOL BLUE	58
XIII	TIME EFFECTS ON TURCO ETCHED Ti 6-4 SURFACE WITH BROMTHYMOL BLUE	59
XIV	TIME EFFECTS ON TURCO ETCHED Ti 6-4 SURFACE WITH THYMOL BLUE	60
XV	COLORS OF THE INDICATORS IN ETHANOL	62
XVI	λ_{MAX} VALUES AND COLOR CHANGES OF THE INDICATORS IN ETHANOL ON TURCO ETCHED Ti 6-4 SURFACE	63
XVII	λ_{MAX} VALUES AND COLOR CHANGES OF INDICATORS IN ETHANOL ON PHOSPHATE-FLUORIDE ETCHED Ti 6-4 SURFACE ...	64

<u>Table</u>		<u>Page</u>
XVIII	TEMPERATURE EFFECTS ON TURCO ETCHED Ti 6-4 SURFACE	68
XIX	TEMPERATURE EFFECTS ON PHOSPHATE-FLUORIDE ETCHED Ti 6-4 SURFACE	69
XX	EFFECTS OF KEEPING HEATED SAMPLES IN AIR AT ROOM TEMPERATURE FOR 90 HOURS	70
XXI	RELATIVE HUMIDITY EFFECTS ON TURCO ETCHED Ti 6-4 SURFACE	72
XXII	RELATIVE HUMIDITY EFFECTS ON PHOSPHATE-FLUORIDE ETCHED Ti 6-4 SURFACE	73
XXIII	EFFECT OF ARGON DRYING ON TURCO ETCHED Ti 6-4 SURFACE	74
XXIV	EFFECT OF ARGON DRYING ON PHOSPHATE-FLUORIDE ETCHED Ti 6-4 SURFACE	75
XXV	ESCA PEAK PARAMETERS FOR Ti 6-4 BEFORE AND AFTER CHEMICAL SURFACE TREATMENTS (66)	77
XXVI	RESULTS OF THE ESCA ANALYSIS OF BARE Ti 6-4 SURFACE, AFTER TURCO AND PHOSPHATE-FLUORIDE PRETREATMENTS	80
XXVII	RESULTS OF THE ESCA ANALYSIS AFTER SPREADING THE BROMTHYMOL BLUE ON PHOSPHATE-FLUORIDE AND TURCO ETCHED Ti 6-4 SURFACES AND BROMTHYMOL BLUE WITH HC1 ON THE Ti 6-4 SURFACE	83
XXVIII	RESULTS OF THE ESCA ANALYSIS OF TURCO AND PHOSPHATE- FLUORIDE ETCHED Ti 6-4 SURFACES AFTER IMMERSING IN BROMTHYMOL BLUE SOLUTION	87
XXIX	RESULTS OF THE ESCA ANALYSIS OF TURCO AND PHOSPHATE- FLUORIDE ETCHED Ti 6-4 SURFACES AFTER IMMERSING IN THYMOL BLUE SOLUTION	88
XXX	MAJOR PEAKS IN THE SPECULAR REFLECTANCE INFRA-RED SPECTRA OF STEARIC ACID ON Ti 6-4 METAL COUPONS	91
XXXI	INTENSITIES OF THE PEAKS IN THE SPECULAR REFLECTANCE INFRA-RED SPECTRA OF Ti 6-4 METAL COUPONS	92

TablePage

XXXII	INTENSITIES OF THE PEAKS IN THE SPECULAR REFLECTANCE INFRA-RED SPECTRA OF PRE-TREATED Ti 6-4 METAL COUPONS AFTER IMMERSION IN 0.001%, 0.01%, AND 0.02% STEARIC ACID SOLUTIONS	94
-------	--	----

LIST OF FIGURES

<u>FIGURE</u>		
	<u>Page</u>	
1 Acid-Base Strength of Magnesium Oxide vs. Heat Treatment Temperature	15	
2 Optical Diagram using the Integrating Sphere for Diffuse Reflectance Measurements	34	
3 Pyrex Custom Apparatus used for Drying the Metal Coupons	38	
4 Unicam Specular Reflectance Attachment	40	
5 Scanning Electron Photomicrographs of Phosphate-Fluoride Etched Ti 6-4 Surface	47	
6 Scanning Electron Photomicrographs of Pasa-Jell Etched Ti 6-4 Metal Surface	48	
7 Scanning Electron Photomicrographs of Turco Etched Ti 6-4 Surface	49	
8 Diffuse Reflectance Visible Spectra of Bromthymol Blue on Phosphate-Fluoride Etched Ti 6-4 Surface	54	
9 Diffuse Reflectance Visible Spectra of Bromthymol Blue on Turco Etched Ti 6-4 Surface	55	
10 Scanning Electron Photomicrographs of Phosphate-Fluoride Etched Ti 6-4 Metal Surface After Exposing to Air at 230°C for 10 Hours	66	
11 Scanning Electron Photomicrographs of Turco Etched Ti 6-4 Metal Surface After Exposing to Air at 230°C for 10 Hours	67	
12 ESCA Photopeaks of Ti 6-4 Surface after Phosphate-Fluoride Pretreatment	78	
13 ESCA Photopeaks of Ti 6-4 Surface after Turco Pretreatment	79	
14 Oxygen 1S Photopeak after Resolving into Two Components on Turco Etched Ti 6-4 Surface	82	
15 The Structures of Acid and Base Forms of Bromthymol Blue	85	

<u>FIGURE</u>		<u>Page</u>
16	Specular Reflectance Infra-red Peaks in the Region 2700-3200 cm ⁻¹ of 0.02% Stearic Acid Adsorbed on Turco and Phosphate Fluoride Etched Ti 6-4 Surfaces ..	96
17	Specular Reflectance Infra-red Peaks in the Region 1600-1800 cm ⁻¹ of 0.02% Stearic Acid Adsorbed on Phosphate-Fluoride and Turco Etched Ti 6-4 Surfaces ..	97
18	Acid Sites on Ti 6-4 Surface after Phosphate- Fluoride Pretreatment	99
19	Acid Sites on Ti 6-4 Surface after Phosphate- Fluoride Pretreatment	100
20	Acid Sites on Ti 6-4 Surface after Phosphate- Fluoride Pretreatment	101
21	Acid Sites on Ti 6-4 Surface after Phosphate- Fluoride Pretreatment	102
22	Functional Groups on Turco Etched Ti 6-4 Surface	104

Chapter I

INTRODUCTION

Titanium 6-4 alloy, introduced in 1954, is a highly stabilized, alpha beta phase alloy, using aluminum (6%) as the alpha stabilizer and vanadium (4%) as the beta stabilizer (1). The general corrosion resistance of titanium and its alloy is superior to many common engineering metals. One of the most important considerations for joining titanium, its alloys, and indeed many metals by adhesive bonding is the difficulty of removing contamination. A variety of specialized surface treatments for Ti 6-4 have been developed over the past decade to remove contamination and thus improve the adhesive bonding.

It is important in this respect to understand the forces involved in adhesive bonding. It has been suggested that intermolecular interactions consist only of dispersion forces and acid-base interaction for the systems consisting of organic acids and bases. The dipole interactions (other than those which are measured as part of acid-base interactions) were considered to be negligibly small (2). This principle has been extended (3) to the work of adhesion (W_A)

$$W_A = W_A^d + W_A^{AB}$$

where W_A^d is that part of the work of adhesion contributed by dispersion forces, and W_A^{AB} is the part contributed by acid-base interaction.

In addition to adhesion, acid-base properties of solid surfaces play an important role in ion exchange and heterogeneous catalysis (4).

Extensive investigations (5) of solid acid catalysts over the last thirty years have resulted in major contributions to both fundamental research and industrial development. However this work has been restricted to high surface area solids such as powders like aluminas and silicas.

There are many instances where we deal with low surface area solids such as the substrates used in adhesion and coatings. Less work has been done in the past on acid-base properties of these low surface area solids. However it is important to realize that measurements of surface acidity would be extremely useful in the areas of adhesion and corrosion.

The objective of this work was to investigate the acid-base properties of titanium 6-4 plates (low surface area) after three different pretreatments, namely Turco, phosphate-fluoride and Pasa-Jell. A series of indicators was used and color changes were detected using diffuse reflectance visible spectroscopy. Electron spectroscopy for chemical analysis (ESCA) was used to examine the indicator on the Ti 6-4 surface. Specular reflectance infra-red spectroscopy was used to study the adsorption of stearic acid from cyclohexane solutions on the Ti 6-4 surface.

Chapter II

LITERATURE SURVEY

This section covers the literature survey related to acid-base characteristics of solid surfaces.

(A) Acid Base Theories

There are many definitions of acids and bases reported in the literature, notably those of Arrhenius, Franklin, Bronsted, German, Lewis, Ussanowitch, Bjerrum, Johnson, Lux, Flood et al. and Tomlinson, Shatenshtein, and Pearson (4). The Bronsted and Lewis theories are mainly used today.

According to Bronsted in 1923, "an acid is a species having a tendency to lose a proton, and a base is a species having a tendency to add on a proton". This can be represented by



where A and B are the acid and conjugate base, respectively (6). The symbol H^+ represents the proton and not the 'hydrogen ion' of variable nature existing in different solvents, so that the definition is independent of the solvent.

The term 'acid' is often used today in a different sense, as was first proposed by G. N. Lewis. A Lewis acid is defined as a species which can accept an electron pair with the formation of a covalent bond, and typical examples are BF_3 , Ag^+ and SO_3 . Similarly, a base is defined as a species which can donate an electron pair with the formation of a

covalent bond. Since such species can accept protons, the Bronsted and Lewis definitions of bases will comprise the same species. However this is not the case for the definition of acids, since Bronsted acids always contain protons, while Lewis acids need not and usually do not.

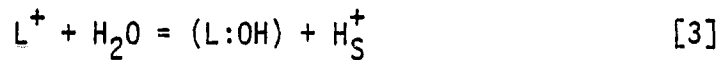
The acid-base concept for a solid surface is complicated because there are two forms of acid sites, namely Lewis and Bronsted acid sites (7). As with a molecular Lewis acid, a Lewis acid site on a solid is a site which has an unoccupied orbital with a high affinity for an electron pair. A major decrease in energy is obtained when such a site shares an electron pair donated by a base molecule. However, the acid strength of a site by this definition is not solely determined by its electron affinity, but includes other factors such as the geometry of the site and orientation of the unoccupied orbitals. In other words improper orientation of the unoccupied orbitals leads to no adsorption of the base molecule. Lewis base sites on the surface can also arise which have electron pairs available at a higher energy level, and a major decrease in energy is obtained if they share this electron pair with an adsorbed pair acceptor.

A Bronsted acid site has a tendency to give up a proton. The acid strength, or acidity of a Bronsted site on a solid is indicated by its ability to drive equation [2] to the right.



where B is the base molecule, BH^+ is its conjugate acid form, and H^+ is the proton provided by the Bronsted site.

In many cases both Lewis and Bronsted acid sites can be related by the presence of water.



where L^+ , the Lewis site, a cation on the surface, shares an electron pair with the OH^- ion from the water molecule, and the remaining proton H_S^+ is adsorbed but easily removed in a chemical reaction. Thus a Lewis acid site has been converted to a Bronsted site.

(B) Indicator Theories and Indicator Method

Acid-base indicators are substances which undergo some marked and sharply defined visual change such as color, fluorescence or turbidity, depending on the acidity or alkalinity of a solution. The history of indicators dates back to 1767 (8).

There are several theories in the literature which have been used to account for the observed color changes of the indicators. Two concepts have appeared most plausible. They are the ion theory or the theory of Wilhelm Ostwald and the chromophore or chemical theory which is usually referred to as the theory of Hantzsch (9).

According to Ostwald, acid-base indicators are weak acids or bases which, when undissociated, exhibit a color different from the ionic forms (9). Even though the original views of Ostwald are not entirely correct, the expressions derived by him still apply to an indicator which behaves like a mono basic acid.

Some of the defects in Ostwald's theory led to the development of the so called chromophore theory or the theory of Hantzsch (8).

Hantzsch and his co-workers have shown that the color change is not due to ionization, but rather results from structural changes. The theory of Hantzsch allows a better explanation of the mechanism of indicator color change than does that of Ostwald. However it is not capable of quantitative treatment. Kolthoff combined the two theories and introduced the unified Ostwald-chromophore theory (8).

According to Kolthoff acid-base indicators may be defined in the following way: "acid-base indicators are apparently weak acids or bases, the ionogenic (aci- or baso-) forms of which have a different structure and so a different color from the pseudo-form" (9). In the case of indicator acids, the color change is regulated by the equilibrium between the ionogenic aci-(A) and pseudo-(P) forms followed by the electrolytic dissociation of the aci-form. This could be described as follows.



where K' is the equilibrium constant for the equilibrium between the pseudo- and aci- forms. For the dissociation reaction of the aci- form



where K_A represents the normal electrolytic dissociation constant of the aci- form. Combining equations [5] and [7]

$$K_A = [H^+][A^-]/K'[P] \quad [8]$$

$$K_A K' = [H^+][A^-]/[P] \quad [9]$$

for which

$$[H^+] = K_i[P]/[A] \quad [10]$$

where K_i represents the apparent dissociation constant of the indicator acid. Consequently the color of the indicator changes with the hydrogen ion concentration according to equation [10]. This description is similar to Ostwald's original views.

The color changes of the indicators as effected by variation of the pH can also be explained by the phenomenon of 'resonance'. This is known as the 'Resonance Theory' (8). Systems having chromophore and auxochrome groups have loosely bound electrons. If the loosely bound electrons of such groups interact, the system will show resonance. The electrons can be activated easily, thus the absorption of light may fall in the visible region of the spectrum. Color changes can occur if the number of possible mesomers or resonance forms change: for instance, if the unshared electron pair of one of the auxochrome groups becomes bound by a proton. Using this phenomenon, Schwarzenbach gave the following definition for the indicators: 'indicators are those acids and bases in which considerable change will occur in the distribution of electrons if the molecule donates or accepts a proton' (8).

The use of indicators to determine the acidity of solid surfaces

was originally reported by Walling (10), Weil-Malherbe and Weiss(11). This method which is known as the visual color change method has been used extensively by many other workers (4). Walling observed the color changes of different indicators adsorbed from non-polar solvents onto solid powders. The results are given in Table I. This visual color change method has also been used to study the solution chemistry within stress corrosion cracks, using indicator - impregnated filter paper, and indicator-coated silica gel (12). The color changes observed after placing the silica gel coated with bromcresol green on the fracture surface of Al and Ti alloy specimens suggested local variation in the acidity. The individual silica gel particles ranged in color from yellow characteristic of pH 3.8 to blue characteristic of pH 5.4 along the fracture surface.

Studies have also been made to characterize the absorption spectra of indicators adsorbed on alumino-silicates surfaces (4). The maximum wavelength in the absorption spectra of the adsorbed indicators has been compared with the maximum wavelength of acidic and basic forms of the indicators. This has been used to identify the form of the indicator present on the surface and thus to determine the acid-base strength of the surface. Alumino-silicates were found to be acidic by this method. This spectrophotometric method has also been used to determine acid-base properties of montmorillonite (13).

(C) Acid Strength and Hammett Acidity Functions

There is always a problem of measuring acidity and basicity of a substance or a solution, due to medium effects, such as solvent

TABLE I
COLORS OF THE INDICATORS ADSORBED ON VARIOUS SOLIDS (10)

Solid	p-dimethylamino azobenzene	1-4 di-(iso-propyl amino-) anthraquinone	Benzeneazodi phenylamine
TiO ₂	Y	B	-
Mg(ClO ₄) ₂	R	-	V
CuSO ₄	R	R	V
Silica gel (Davco)	R	R	V
Alumina (Fisher)	Y	B	Y

B = Blue; R = Red; V = Violet; Y = Yellow

acidity and dielectric constant (14). To overcome this problem, Hammett and Deyrup first proposed the concept of the 'acidity function' H_0 (15). This was applied to determine acid strength of solutions whose acidity lies between that of dilute solutions and 100% sulfuric acid (16). A series of structurally similar indicators were used for this study.

A simple indicator is defined as a non-ionized or neutral substance capable of adding one hydrogen ion per molecule without any complicating further reactions. Color change is determined by the extent of the reaction [11].



$$K^\infty = \lim_{C \rightarrow 0} \frac{[H^+][B]}{[BH^+]} \quad [12]$$

One indicator (B_1) should be chosen such that it is a strong enough base to permit the determination of $[B_1]/[B_1H^+]$ in aqueous solution. For this K^∞ could be estimated from equation [12] with satisfactory precision. A second indicator (B_2) should be chosen such that, its $[B_2]/[B_2H^+]$ ratio can be measured within a higher acidic range than the first one, but also having an overlapping region with the first indicator. Thus, if the ionization ratios $[B_1]/[B_1H^+]$ and $[B_2]/[B_2H]$ for the two indicators are measured in a given solution, it could be described by the equation [13].

$$\begin{aligned} pK_{B_1} - pK_{B_2} &= -\log[B_1][B_2H^+]/[B_2][B_1H^+] - \log f_{B_1} \cdot f_{B_2H^+}/f_{B_1H^+} \cdot f_{B_2} \\ &\quad A \qquad \qquad \qquad B \quad [13] \end{aligned}$$

where f_{B_1} , $f_{B_1H^+}$, f_{B_2} and $f_{B_2H^+}$ are the activity coefficients of B_1 , B_1H^+ , B_2 and B_2H^+ respectively. The first term A on the right hand side can be measured colorimetrically. For structurally similar indicators, it is assumed that the activity coefficient term B on the right hand side is zero. Thus with the known value of pK_{B_1} , the pK_{B_2} value can be calculated using equation [13]. If we have a series of simple basic indicators covering any range of acidities, by a stepwise application of the this procedure, pK values could be calculated.

The Hammett acidity function is defined by equation [14]:

$$H_o = \log [B]/[BH^+] + pK_B \quad [14]$$

It may be interpreted as a measure of the extent to which a base reacts with hydrogen ion in a given solution. It is also equivalent to

$$H_o = -\log a_{H^+} \cdot f_B / f_{BH^+} \quad [15]$$

where a_{H^+} is the proton activity.

The scope and success of the H_o function treatment of acidity in homogeneous media suggests a similar definition for the acidity of a solid surface (10). According to Walling, acid strength of a solid surface is the ability of the surface to convert an adsorbed neutral base into its conjugate acid. In the case that the conversion involves the usual proton transfer, this permits the assignment of an H_o function for the surface expressed by equation [15].

If the reaction takes place by means of electron pair from the adsorbate to the surface, H_o is expressed by

$$H_o = -\log a_A \cdot f_B / f_{AB} \quad [16]$$

which can be rewritten as

$$H_o = pK_a + \log [B] / [AB] \quad [17]$$

where a_A is the activity of the Lewis acid or electron pair acceptor and the pK_a term includes the activity coefficients.

The visual color change method could be used to measure H_o values of surfaces. The color of suitable indicators adsorbed on a surface will give a measure of its acid strength. If the color of the indicator adsorbed on the surface is the same as that of the acid form of the indicator, then the value of H_o function of the surface is $\leq pK_a$ of the indicators. Acid strengths determined by this method are given in Table II (4). The same idea has been developed to obtain representative parameter $H_{o,\max}$ of acid-base strength on solid metal-oxygen compounds (17).

The base strength of a solid surface is defined as the ability of the surface to convert an electrically neutral acid to its conjugate base (4). For the reaction of an indicator AH with a solid base B



The base strength H_o of B is given by an equation [19] similar to

TABLE II
ACID STRENGTH OF SOME SOLIDS (4)

Solids	H_o
Hydrogen kaolinite	-5.6 ~ -8.2
Montmorillonite	+1.5 ~ -3.0
$SiO_2 \cdot Al_2O_3$	< -8.2
1.0 mmol/g H_3BO_3/SiO_2	+1.5 ~ -3.0
$NiSO_4 \cdot xH_2O$ heat-treated at $350^\circ C$	+6.8 ~ -3.0
ZnS heat-treated at $300^\circ C$	+6.8 ~ +4.0
TiO_2 heat-treated at $400^\circ C$	+6.8 ~ +1.5

equation [17].

$$H_o = pK_a + \log [A^-]/[AH] \quad [19]$$

where $[AH]$ is the concentration of the acidic form of the indicator, and A^- is the concentration of the basic form. Acid-base strengths of magnesium oxide prepared by heating the hydroxide were measured using this method (4). The results are shown in Figure 1. Here the base strength decreases as the temperature is raised.

(D) Other Methods Used in the Determination of Acid-Base Properties of Surfaces

There are various methods reported in the literature (5) to assess the acidity of solid surfaces. These can be summarized as follows:

1. Aqueous methods
2. Non aqueous liquid phase methods
3. Adsorption from gas phase
4. Hydrogen-deuterium exchange reactions
5. Optical spectroscopy.

1. Aqueous methods

When a solid is slurried in water, the pH of the solution phase changes. Acidity or basicity of the surface can be determined by titrating the slurry or portion of solution phase with a standard base solution. Attempts have been made to determine acidities of silica-alumina slurries in water by titrating with sodium hydroxide (5). The end point was established in a few minutes, when the slurry was

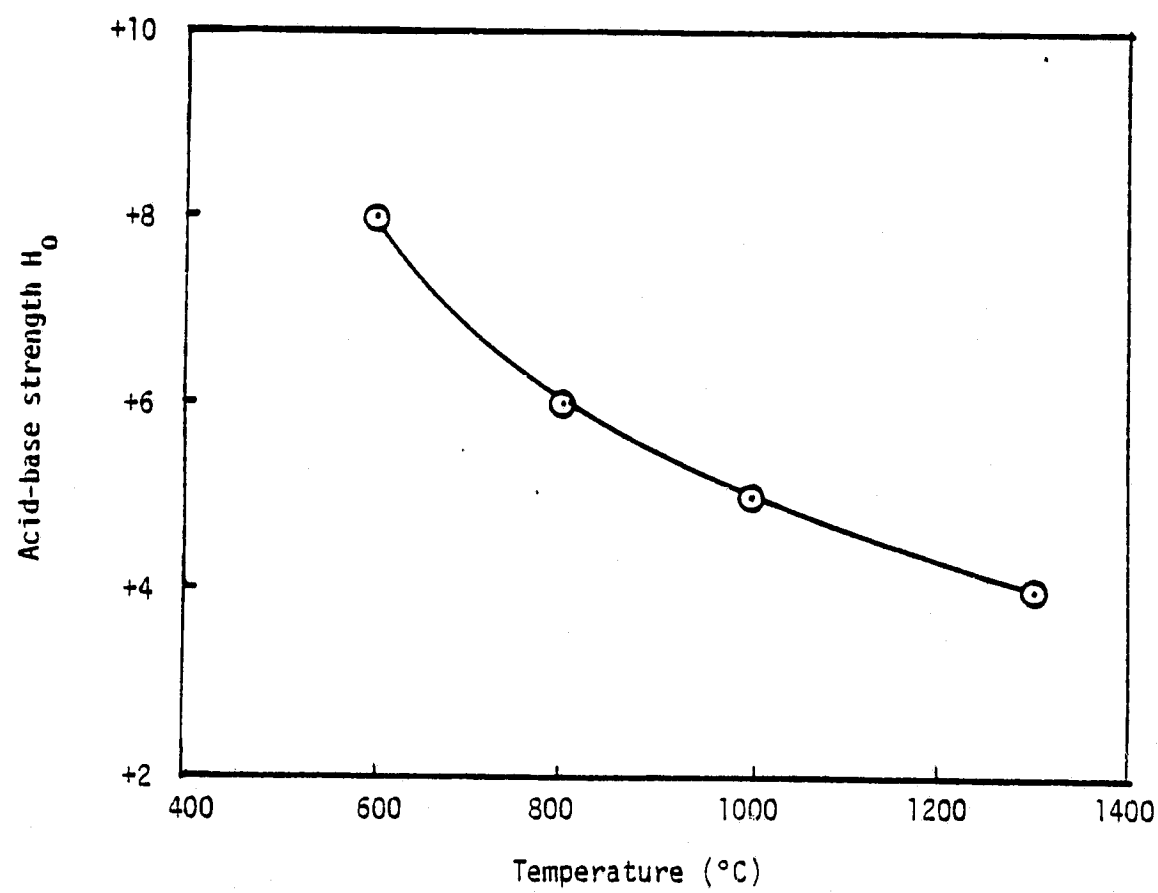


Figure 1. Acid-base Strength of Magnesium Oxide vs. Heat Treatment Temperature (4)

titrated immediately. However more base was required to establish the end point when the titrated slurry was allowed to stand for a period of hours.

Ion exchange reactions of cations on the surfaces including hydronium and hydroxyl ions have been used to measure the acidity of surfaces. Ammonium ions have been exchanged with hydronium ions and from the degree of exchange, the protonic acid content on silica-alumina catalyst at various compositions has been calculated (18). Maximum protonic acid content of 0.80 meg/g was found at a SiO_2 composition of 82% by weight.

2. Non aqueous liquid phase methods

Titration of a standard solution with adsorbed indicators was reported first by Tamale (4) and Bensi (5). The indicator changes color when adsorbed on the acid surface from non aqueous solvents. Thus the amount of amine required to restore the original color give a measure of number of acid sites on the surface. The convenience of this method has lead to its extensive use by many workers (4). Titration of n-butyl amine with benzene as the solvent has been used to determine the surface acidity of nickel sulfate powder (19). The surface acidity of cation exchanged Y-Zeolites (20), has been determined by means of amine titrations, observing color changes of adsorbed indicators in the H_0 range +6.8 to -8.2 in benzene solution. The surface acidity of titanium oxides (21) has also been measured by titration with amine. Attempts have also been

made using benzylamine to determine acidities of silica-alumina surfaces suspended in carbon tetrachloride and iso-octane (22). The acidities of various silica-alumina catalysts were found to be in the range of 0.09-0.58 meq/g. Iso-octane has also been used as the solvent with titrating bases ethylene diamine, quinoline and pyrrole (5). Difficulties in establishing adsorption equilibrium in n-butylamine titration of solid acid surfaces are also reported (23). Attempts have been made to measure surface acidity of silica-alumina by titrating with indicator itself (24). The acid content measured by the direct titration method was less than with the butylamine titration method. This difference has been ascribed to the difference in the base strength of titrants.

The number of basic sites on a surface can be determined by titrating an adsorbed indicator on a basic solid with an acid. The base strength of CaO and slags such as $\text{SiO}_2\cdot\text{CaO}\cdot\text{MgO}$ suspended in benzene have been measured by titrating the adsorbed bromthymol blue indicator with benzoic acid (4). The basicity of $\text{SiO}_2\cdot\text{CaO}\cdot\text{MgO}$ varied from -5.7 to +3.7 $\frac{\mu\text{mol}}{\text{g}}$ depending on the composition. Trichloro acetic acid has also been used as a titrant to determine acid-base strength distribution on solid surfaces (25). It was found by this method that the basic sites of selected solids at basic strengths for which $H_o > 1.5$ has the order $\text{ZnO} > \text{TiO}_2 > \text{Al}_2\text{O}_3 > \text{BaO} > \text{activated Al}_2\text{O}_3 > \text{B}_2\text{O}_3 > \text{ZrO}_2 > \text{MgSO}_4 > \text{MoO}_3$.

Attempts have been made to follow the titrations potentiometrically. This method has been used to measure acidities of catalyst powders

which were slurried in acetonitrile by titrating with n-butyl amine (5). By the signal from a glass electrode, the course of titration has been followed. Studies have also been reported on the distribution of surface acid strength of carbon black by potentiometric titration (26). It was found that the weaker acid sites with pK_a values between 7.0 and 11.0 occur in the amount 0.025-0.490 meq/g, while stronger acid sites with pK_a range of 2.0 to 7.0 occur in the amount 0-0.475 meq/g.

The acid amount of colored solids can also be determined by calorimetric titration. In this method, the increase in temperature with the addition of the base titrant is determined. This has been used to measure acid strength of silica-alumina by titration with n-butylamine (4). The acid amount was found to be 0.78 $\mu\text{mol/g}$.

Direct measurement of heats of wetting of solid samples in n-butylamine has also been used to measure acidity of surfaces (5). It was found that the differential heats of adsorption for kaoline-pelletized catalyst K-2 is in the range -4.0 to -10.0 kcal/mole for the surface coverage of 0-0.8. These values reflected the acid strength distributions.

AdSORptive properties of polymers such as polymethylmethacrylate (PMMA) and polyvinyl chloride (PVC) from organic solvents on to acidic and basic inorganic powders have been used to determine acid-base properties of polymers (3). The results showed that the PMMA was basic while PVC was acidic.

3. Adsorption from gas phase

When gaseous bases are adsorbed on acid sites, it is more difficult to desorb the base adsorbed on strong sites than the one adsorbed on weak acid sites. Thus the amount of adsorbed base after different desorption methods will give the indication of acidity of surface. Numerous desorption methods have been used including the following:

- a) Thermal desorption into vacuum (27).
- b) Thermal desorption in a closed system (28).
- c) Flash desorption into a carrier gas stream (5).

Gaseous bases which have been mainly used are ammonia, pyridine, quinoline, piperidine, trimethylamine, n-butyl amine and pyrrole (5,4). In addition, work has also been reported with diborane, carbon dioxide, and hydrogen sulfide (4). Gravimetric analysis, differential thermal analysis, thermal gravimetric analysis, volumetric and chromatographic techniques and heats of adsorption have been used to determine the amount of gas adsorption (4,5).

Gaseous adsorption method can also be used to measure basicities of surfaces. Basicities of oxide surfaces such as CaO, BeO, MgO, ZnO, silica gel and alumino silicates have been determined by phenol vapor adsorption (4). Attempts have also been made to use boron trifluoride as the adsorbate in the determination of basic sites in alumina semiconductors doped with different cations (5). The number of carbon dioxide molecules adsorbed per unit surface area has also been considered as a measure of the number of basic sites on the surface (29). It was found that the steaming of magnesia

did not result in the formation of additional basic sites for CO_2 adsorption.

4. Hydrogen-deutrium exchange reactions

One way to probe the nature of the acid sites on catalyst surfaces is to study reactions of hydrogen on these surfaces (5). Several of these involve exchange reactions with deuterium.

Differential hydrogen analysis is a technique to distinguish between different kinds of hydrogen on a surface. In this method deuterium exchange rates at different temperatures are measured. These studies have been done on alumina, silica and silica-alumina surfaces (5).

Relative rates of hydrogen exchange in reactant molecules and on the surface are also used to distinguish between reactive and non reactive surface hydrogens. This is known as the method of competitive exchange reactions. Hydrogen-deuterium exchange reactions between CH_4 and deuterated catalysts and between CD_4 and hydrogenated catalysts have been studied (30). By the CD_4 exchange method the hydroxyl content of an alumina catalyst was found to be $2.6 \times 10^{14}/\text{cm}^2$.

5. Optical spectroscopy

Information about surface acidity from optical spectroscopy has come from studies of hydroxyl groups and adsorbed molecules on the surfaces. The infra-red region has been used in both kinds of studies. Other techniques were mostly used in studies of adsorbed molecules.

Several studies are reported on the study of nature of hydroxyl groups on surfaces by infra-red spectroscopy (5). The nature of hydroxyl groups is related to surface acidity and basicity. It has been observed that, silica, alumina and silica-alumina surfaces have different kinds of hydroxyl groups and thus different acid-base characteristics (31).

Infra-red studies of ammonium ions and ammonia adsorbed on clay samples have been used to estimate the amount of Bronsted and Lewis sites on clay samples (5). Similar kinds of studies are reported on pyridine adsorbed on silica-alumina (5), Ge near-faujastic zeolite (32) and Y-zeolites (33). 2-4 disubstituted pyridines have also been used as probe molecules in studying the acidities of surfaces by infra-red spectroscopy (34,35). The acidic properties of silica-alumina gels have been studied as a function of chemical composition with pyridine and CD_3CN as adsorbing molecules (36). Studies are also reported on the use of hydroxyl band frequency shifts of phenols, in determining acidities of oxide surfaces (37).

Most of the ultra-violet spectroscopic studies are directed at distinguishing between Bronsted and Lewis acid sites (5). Ultra-violet spectroscopic studies of adsorbed triphenyl carbonium ions have been used to determine acid-base characteristics of silica-alumina catalysts (5). Acid properties of aluminum oxide surfaces have been studied by ultra-violet spectra of deposited metals (38).

Studies have been reported on photo electron spectroscopy in the determination of acid-base characteristics of ammonium Y-zeolite surfaces (33) and $\text{SiO}_2\text{-Al}_2\text{O}_3$ gels (39). A binding energy difference

of 2 ev was found between the N1s level of pyridine before and after the adsorption on ammonium Y zeolite.

ESR and diffuse reflectance spectra of adsorbed polyacenes have been used to study acidic properties of silica-gel, alumina and silica-alumina (40). Attempts have also been made to study acidity of alumina and gallium oxide surfaces by electron paramagnetic resonance (41). Studies on laser-Raman spectra of adsorbed pyridine molecules have been used in the determination of acidity of oxide surfaces (42). Investigation of the surface acidity of silica-alumina and mixed silica-alumina by carbon-13 NMR of adsorbed amines is also reported (43).

(E) Characterization Techniques

Only a few studies have been reported on diffuse reflectance visible -ultra violet spectroscopy (DRVS). Discussion here will be on adsorbed organic molecules on solid surfaces.

The DRVS technique has been used to study electronic changes occurring in MgO after exposure to CO, NO₂ and C₂H₂ (44). The formation of anionic clusters like (CO)₂²⁻ and (CO)_n^{X-} were observed on the MgO surface. Studies have also been reported on DRVS of pyroxenes on solids (45). It was found that the wavelength of bands vary as a function of pyroxene composition. Formation of charge transfer complexes by solid-state reactions has been studied for donors like naphthalene and acceptors like benzoquinone by DRVS (46). It was observed that the relative reactivity depended directly on the molecular size and geometry. Studies have also been reported on the DRVS of

heteropolyanions containing two different hetero atoms (47). It has been found that the salts whose reflectance and solution spectra differ markedly were dichroic. DRVS of 1:1:1 α -naphthyl amine -pyridine-picric acid complex has been studied (48). It has been found that transfer of proton from picric acid to pyridine takes place in the complex formation.

Theoretical calculations have also been reported on DRVS. Values of Slater-Condon, Racah, Lande bonding and screening parameters have been calculated from DRV spectra of trisneodymium sulfate (49). Progress of theoretical aspects of DRVS have also been discussed (50).

Electron spectroscopy for chemical analysis (ESCA) and reflectance infra-red spectroscopy (RIRS) have been extensively used by many workers. The discussion here will be restricted to studies of organic molecules on metal surfaces.

Decomposition of formic acid on Ni, Cu and Au surfaces has been examined by ESCA (51). The existence of formate ion has been established on all the surfaces. The temperature dependence of the interactions of formic acid with polycrystalline Cu, Ni and Au has also been examined (52). It has been found that formate ion decomposition on different surfaces occurred at different temperatures. ESCA studies have also been reported on adsorption of vinyl chloride and alkenes on Pt surfaces (53). Dissociative chemisorption of vinyl chloride at low coverages and associative chemisorption of alkenes, on Pt surfaces were observed. Extended Huckel molecular orbital studies in ESCA have also been used to examine the dissociative

chemisorption of C_2 , ethylene on tungsten and nickel surfaces (54).

Studies in ESCA have also been reported on surface compounds formed on Cu_2O and CuO immersed in benzotriazole (BTA) (55). Formation of Cu^{+2} -BTA has been observed on the surface. ESCA has also been used to study the adsorptive properties of gaseous methanol flowing over tungsten surfaces where chemisorption of methanol on tungsten has been observed (56). Electron beam effects on condensed multilayers of homologous series of H_2O , CH_3OH and $(CH_3)_2O$ on $Ni(100)$ crystals have also been studied using ESCA (57). The results indicated the presence of new chemical species by electron damage. ESCA has also been used to study the decane adsorption on aluminum (58). Surface plasmon satellites were observed in the C1s photo-peaks. This indicated the presence of a thin oxide layer on the surface.

Reflectance infra-red studies have been done on the chemisorption of C_2H_2 and C_2H_6 on evaporated Ag and Pt surfaces (59). Formation of acetylenic and saturated species has been observed. Studies have also been reported on polarised attenuated total reflectance measurements of Ge electrodes from aqueous solutions of sodium laurate (60). Adsorbed layers were found to be an assembly of monoclinic crystallites of lauric acid. Surface transport of stearic acid on $\alpha-Al_2O_3$ has been studied using reflectance infra-red spectroscopy (61). The nature of co-adsorbed molecules like water and methanol were found to have a greater effect on the surface transport.

Chapter III

EXPERIMENTAL

This section contains a description of the materials used and experimental procedures for the various techniques.

(A) Materials

1. Indicators

Powdered solids were studied using the indicators benzeneazodiphenyl amine, methyl violet, methyl red, bromphenol blue, paradimethylaminoazobenzene, alizarin, p-nitrophenol and o-nitrophenol. Structures, pH values at the color transition, colors of the acid and base forms and sources of the indicators are given in Table III.

The indicators bromthymol blue, thymol blue, bromphenol blue, bromcresol purple, bromcresol green, orange 1 and benzeneazodiphenyl amine were used in the study of low surface area titanium metal coupons. Structures, pH values at color transition, colors of the acid and base forms and sources of the indicators are given in Table IV.

2. Solvents

Toluene, methanol, cyclohexane, iso-octane, 100% ethanol and deionized water were used as the solvents for the indicators which were used to study the powders. Indicator solutions used in the study of the titanium 6-4 metal coupons were prepared with the solvents deionized water and iso-octane.

TABLE III
INDICATORS USED IN THE STUDY OF SOLID POWDERS

Indicator	Structure	Color of the acid form	Color of the base form	pH at color transition	Source
Benzene azo diphenyl amine	$4C_6H_5N:N:C_6H_4NHC_6H_5$	Y	Y	1.2-2.5	Eastman
Crystal violet		Y	B		Fisher
Methyl red		R	Y	4.4-6.2	
Bromophenol blue		Y	B	3.0-4.6	Thomas

TABLE III (continued)

Indicator	Structure	Color of the acid form	Color of the base form	pH at color transition	Source
Methyl yellow		R	Y	2.9-4.0	Aldrich
Alizarin		Y	R	5.5-6.8	Fisher
O-Nitro phenol		C	Y	5.0-7.0	
P-Nitro phenol		C	Y	5.6-7.6	Fisher

B = Blue; C = Colorless; R = Red; V = Violet; Y = Yellow

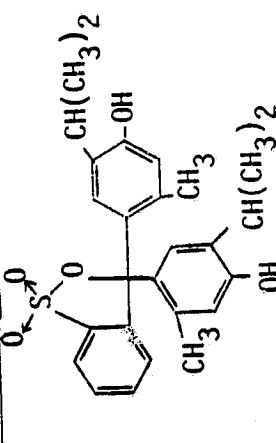
TABLE IV
INDICATORS USED IN THE STUDY OF Ti 6-4 METAL COUPONS

Indicator	Structure	Color of the acid form	Color of the base form	pH at color transition	Source
Benzene azo diphenyl amine	$4C_6H_5N:NHC_6H_5NHCC_6H_5$	V	Y	1.2-2.5	Eastman
Brom phenol blue		Y	B	3.0-4.6	Thomas
Brom cresol green		Y	B	3.8-5.4	Fisher

TABLE IV (continued)

Indicator	Structure	Color of the acid form	Color of the base form	pH at color transition	Source
Brom cresol purple		Y	B	5.2-6.8	Chem. Dynamics
Brom thymol blue		Y	B	6.0-7.6	Chem. Dynamics
Orange !		0	V	7.6-8.9	Pfaltz

TABLE IV (continued)

Indicator	Structure	Color of the acid form	Color of the base form	pH at color transition	Source
Thymol blue		Y	B	8.0-9.6	Pfaltz

3. Solid materials

The powders used in this study were titanium dioxide (TiO_2 -I) obtained from Dr. G. D. Parfitt of Tioxide International, anhydrous $Mg(ClO_4)_2$ and titanium dioxide (TiO_2 -II) obtained from the Cabot Corporation. Titanium 6-4 metal coupons were obtained from personnel at the NASA-Langley Research Center.

4. Materials used in the pretreatment

Hydrofluoric acid and methyl ethyl ketone were obtained from J. T. Baker Co. Nitric acid was obtained from the Allied Chemical Corp. Trisodium phosphate was obtained from the Mallinckrodt Corp. The Turco powder was obtained from the Purex Corp. Sprex-AN and Pasa-Jell were provided by personnel at the NASA-Langley Research Center.

5. Adsorbates

Laboratory grade stearic acid was obtained from Fisher.

(B) Visual Color Changes of the Indicators on Powders

Indicator solutions were prepared by dissolving 1 mg of the indicator in 10cc of the solvent. Color changes of the adsorbed indicators on the solid surface were observed by adding 2 ml of the indicator solution to 1 mg of the solid powder.

(C) Determination of Maximum Wavelength of Absorption of the Indicators

Visible absorption spectra for the different indicator solutions were taken in the wavelength range 350-700 nm, using an Hitachi

100-60 spectrophotometer. The maximum wavelength of absorption for the indicator was determined by the absorption spectra. Measurements were taken for both acid and base forms of the indicators. The base forms of the indicators were obtained by addition of NaOH pellets to the indicator solutions. The acid forms of the indicators were obtained by mixing hydrochloric acid with the indicator solutions. The visual colors of both acid and base forms of the indicators were also noted.

(D) Preparation of Titanium 6-4 Metal Coupons and Indicator Solutions

Three surface pretreatments, namely Turco, phosphate-fluoride and Pasa-Jell were carried out using procedure given in Appendix I.

The indicator solutions were prepared by dissolving 0.01g of the indicator in 25 ml of the solvent. The indicators orange 1 and sodium salts of thymol blue, bromphenol blue, bromcresol green were dissolved in deionized water. The sodium salt of bromcresol purple was prepared by adding 9.25 ml of N/50 sodium hydroxide to 0.1 g of indicator powder. This was diluted to 250 ml with deionized water. The aqueous solution of the indicator bromthymol blue was directly obtained from Chemical Dynamics Corp. The indicator benzeneazodiphenylamine was dissolved in iso-octane.

Soon after the pretreatments of the Ti 6-4 coupons, 6 drops (0.3 ml) of the freshly prepared indicator solutions were placed on the metal surfaces. The indicator solutions were spread over an

area of about 6 cm² and visual color changes were noted within 15-30 minutes. The metals were partially covered with a beaker and allowed to dry for 4 hours. Reference samples were prepared by spreading 6 drops of the solvent which was used to prepare the indicator solution on the Ti 6-4 coupons. When the sodium salt of the indicator was used, the reference samples were prepared by spreading 6 drops of solution containing 7 ml of N/50 sodium hydroxide and 250 ml of water on the Ti 6-4 coupons. Visible diffuse reflectance spectroscopic measurements on the metal samples were made immediately after drying.

(E) Visible Diffuse Reflectance Spectroscopy

A Cary 14 spectrophotometer was used to obtain the visible diffuse reflectance spectra. The optical diagram using the integrated sphere for diffuse reflectance measurements is shown in Figure 2.

The radiation from the illuminating source is diffusely reflected within the sphere resulting in diffuse illumination of the sample and the reference material. Radiation reflected from the sphere is directed to the spectrophotometer chopper, monochromator and detector.

The spectrophotometer was allowed to equilibriate for 24 hours before taking the spectra. The pre-treated metal with the indicator was placed on the sample port and the reference sample was placed on the reference port. The spectra were taken in the wavelength range 700-350 nm with a speed of 10 nm per second within the absorbance range 0-2.

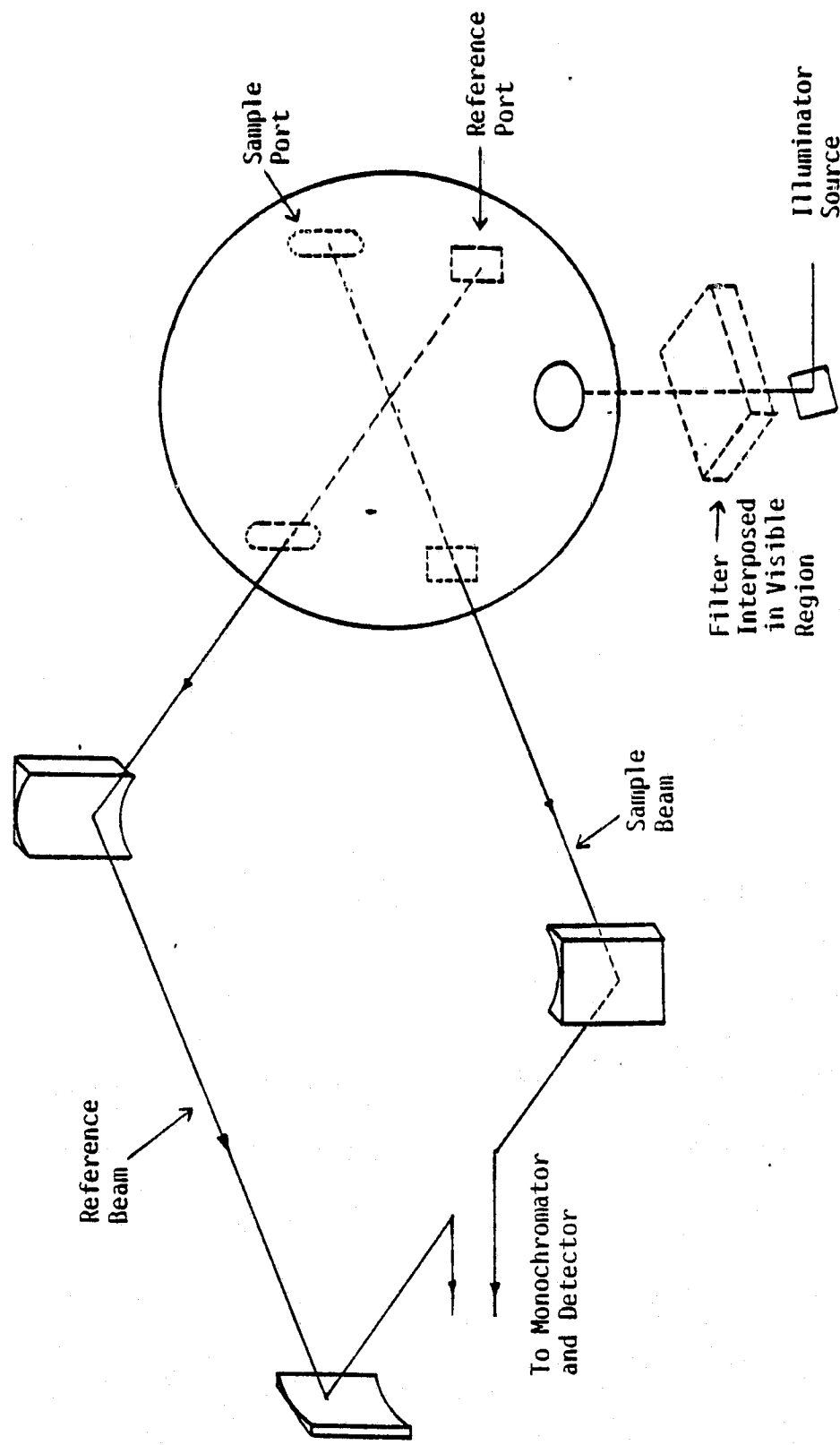


Figure 2. Optical Diagram using Integrating Sphere for Diffuse Reflectance Measurements

(F) Variations of the Experimental Conditions

For all the experiments discussed under this section, the metals were pretreated by the Turco process and by the phosphate - fluoride process.

1. Effect of drying time

Fourteen metal pieces were used for each treatment. Half of them were used with the thymol blue indicator solution and the remaining pieces were used with the bromthymol blue indicator solution. After the pre-treatment process, the metal samples were allowed to dry. The indicator solutions were spread on the metal samples after drying 1, 2, 10, 25, 50 and 100 hours. Visual color changes were noted and diffuse reflectance spectra were taken for each sample.

2. Effect of solvent

Fresh indicator solutions of thymol blue (sodium salt), bromcresol purple, bromcresol green (sodium salt) were prepared by dissolving 4 mg of each indicator in 10 cc of ethanol. The pretreated samples were allowed to dry and the indicator solutions were spread on the surface. Visual color changes of the indicators were noted and visible diffuse reflectance spectra were taken after the indicator dried on the surface.

3. Effect of concentration of the indicator solutions

The indicators bromthymol blue, bromcresol purple and thymol blue were used in this study. Indicator solution of bromthymol blue were diluted ten-fold. Bromcresol purple and thymol blue indicator

solutions were prepared by dissolving 1 mg of indicator in 25 cc of water. Visible diffuse reflectance spectra of the indicators on the pre-treated metal surfaces were taken as before.

4. Effect of temperature

After the pretreatments, the samples were placed in an oven at 230°C for 10 hours, a time period used in earlier work (64), and allowed to cool back to room temperature for 5 minutes. The indicator solutions of bromthymol blue and thymol blue were then spread on two of the samples and diffuse reflectance spectra were taken immediately. The other samples were kept for 90 hours at room temperature and diffuse reflectance spectra were taken with bromthymol blue and thymol blue indicators.

5. Effect of relative humidity

An assumed relative humidity of 100% was obtained by keeping a beaker containing water in a closed dessicator. Calcium sulfate was placed in another dessicator to obtain an assumed 0% relative humidity. Samples were kept in the two dessicators for 100 hours. The indicators bromthymol blue and thymol blue were spread on the surfaces immediately after removal from the dessicator and the visible diffuse reflectance spectra of these samples were obtained.

6. Effect of drying environment

Instead of air drying, the pretreated metal pieces were dried in flowing argon for 1 1/2 hours in the custom pyrex apparatus shown in

Figure 3. After drying the metal, the indicator solutions bromthymol blue and thymol blue were spread immediately on the metal surfaces. The color changes of the indicators were observed and diffuse reflectance spectra were taken.

(G) ESCA Measurements

Indicator solutions bromthymol blue and thymol blue were used in this study. Six drops of the indicator solutions were spread on some of the pretreated metal samples and the others were immersed vertically in the indicator solution for four hours. The immersed samples were taken out of the indicator solution and allowed to dry for 10 minutes. The indicators were also spread on metal surfaces on which a few drops of sodium hydroxide or hydrochloric acid had already been spread. Thus both acid and base forms of the indicators were obtained directly on the metal surfaces. Circular (1/4") pieces were cut out of the metal samples for ESCA analysis. Scotch double stich adhesive tape was used to mount the sample on the probe. A Dupont 650 electron spectrometer with Mg K α radiation (1254 ev) was used to characterize the surfaces of the samples. The normal operating pressure for the analyser was about 5×10^{-7} torr.

Narrow scan spectra were taken for the elements C, O, Br, S, Ti and Na. Binding energies of the elements were corrected taking the binding energy of C 1S photopeak due to surface contamination as 284.6 ev (62). The intensities were corrected with published photoionization cross sections (σ) (63). Atomic fractions (A.F.) were

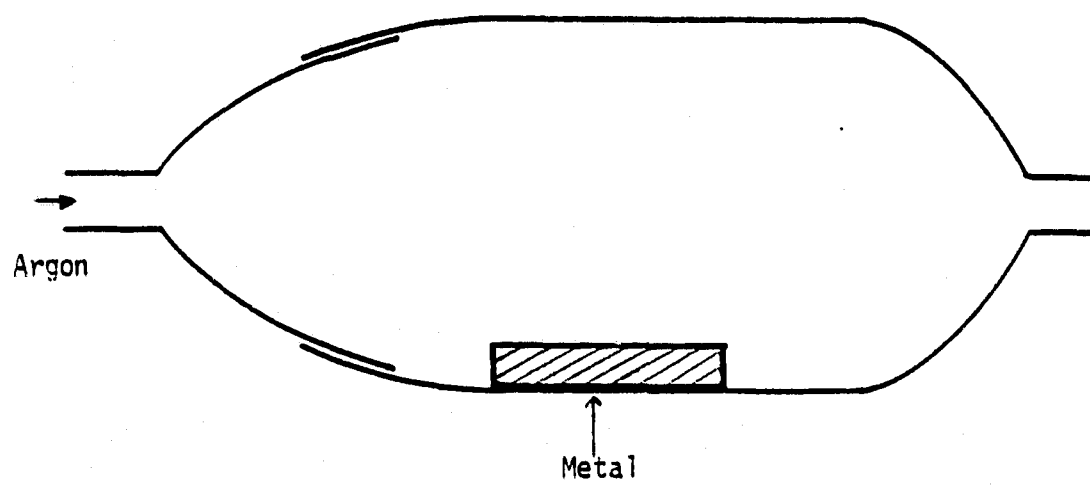


Figure 3. Pyrex Custom Apparatus used for Drying the Metal Coupons

obtained from the equation

$$A.F. = \frac{A_i/\sigma}{\sum A_j/\sigma} \quad [20]$$

where A_i is the area of each significant peak in the ESCA spectrum.

Curve resolution of the unresolved peaks was done on the O 1s photo peaks using GASCAP.

(H) Stearic Acid Adsorption

Four solutions of stearic acid in cyclohexane with concentrations of 0.001%, 0.01% and 0.02% by weight were prepared. The Ti 6-4 samples were pretreated with the Turco process and phosphate-fluoride process and immersed vertically in the stearic solution for one hour. After immersion they were taken out of the solution, placed vertically in separate breakers and allowed to dry. The specular reflectance infrared spectra were taken immediately after drying.

(I) Specular Reflectance Infra-Red Spectra

Specular reflectance infra-red spectra were obtained with a Pye Unicam SP240 specular reflectance unit attached to a Perkin Elmer model 283 spectrophotometer. The specular reflectance unit is based on a single reflection as shown in Figure 4. The specular reflectance infra-red spectra of bare titanium 6-4 after the two pretreatments and after immersing in the stearic acid solutions were taken in the 3000 to 600 cm^{-1} region using an ordinate scale expansion (x10).

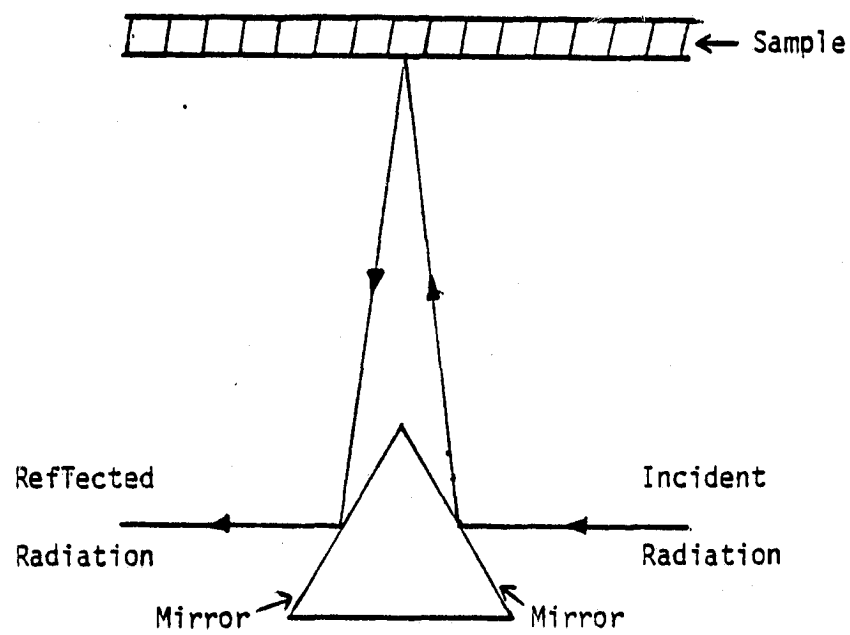


Figure 4. Unicam Specular Reflectance Attachment

Chapter IV

RESULTS AND DISCUSSION

PART I: Study of Solid Powders

Titanium dioxide powders were chosen for study since the presence of an oxide layer on Ti 6-4 surfaces was shown in previous work (64). Solubilities of the indicators in various solvents are tabulated in Table V. $\text{TiO}_2\text{-I}$ and $\text{TiO}_2\text{-II}$ were insoluble and colorless in all the solvents. However both solids formed colloidal suspensions in water, methanol and ethanol. $\text{Mg}(\text{ClO}_4)_2$ powder was soluble in water, methanol and ethanol but insoluble in the other solvents.

When the indicator solutions were mixed with solid powders, immediate adsorption of the indicator was observed. The color changes of the adsorbed indicators were noted and the results are tabulated in Table VI.

The results for the $\text{Mg}(\text{ClO}_4)_2$ powder are in agreement with the results reported by Walling (10). It is apparent that for a given powder the solvent has a significant effect on the observed color changes of the indicators. There are marked differences with the polar solvents. For example, the indicator benzeneazodiphenyl amine in iso-octane changed the color from yellow to violet on $\text{TiO}_2\text{-I}$ but color changes were not observed when the indicator was in ethanol or methanol. In the case of polar solvents, the surface characteristics may have been altered by solvent adsorption. The solid powders $\text{TiO}_2\text{-I}$ and $\text{Mg}(\text{ClO}_4)_2$ were found to be very acidic and

TABLE V
SOLUBILITIES OF INDICATORS IN VARIOUS SOLVENTS

Indicator	Toluene	Iso Octane	Cyclo hexane	Methanol	Water	Ethanol
Benzene azo diphenyl amine	S	S	S	S	I	S
Methyl red	S	PS	PS	S	PS	S
Crystal violet	PS	I	I	S	S	S
Brom phenol blue	I	I	I	S	S	S
Methyl yellow	S	S	S	S	I	S
Alizarin	S	I	I	-	I	S
<i>o</i> -Nitro phenol	S	S	S	-	I	S
<i>p</i> -Nitro phenol	S	I	I	-	PS	S

S = Soluble; PS = Partially Soluble; I = Insoluble

TABLE VI
COLOR CHANGES OF THE INDICATORS ON SOLID POWDERS

Indicator	Solvent	TiO ₂ -I	TiO ₂ -II	Mg(ClO ₄) ₂
Benzene azo diphenyl amine	Iso-Octane	Y→V	Y→Y	Y→V
	Cyclohexane	Y→V	Y→Y	Y→V
	Methanol	Y→Y	Y→Y	Y→Y
	Ethanol	Y→Y	Y→Y	Y→Y
	Toluene	Y→Y	Y→Y	Y→Y
Methyl yellow	Iso-Octane	Y→R	Y→Y	Y→R
	Cyclohexane	Y→R	Y→Y	Y→R
	Methanol	Y→R	Y→Y	Y→P
	Ethanol	Y→Y	Y→Y	Y→P
	Toluene	Y→R	Y→Y	Y→R
Methyl red	Iso-Octane	Y→R	Y→Y	Y→R
	Cyclohexane	Y→R	Y→Y	Y→R
	Methanol	R→R	R→Y	R→Y
	Water	R→R	R→P	R→R
	Ethanol	R→P	R→Y	R→R
	Toluene	Y→P	Y→Y	Y→P
Crystal violet.	Methanol	V→V	V→V	V→V
	Water	V→V	V→V	V→V
	Ethanol	V→V	V→V	V→V
Brom phenol blue	Methanol	B→Y	B→B	B→B
	Water	B→B	B→B	B→B
	Ethanol	B→Y	B→B	B→B
Alizarin	Ethanol	Y→P	Y→R	
	Toluene	Y→P	Y→R	
o-Nitro phenol	Iso-Octane	Y→C	Y→Y	
	cyclohexane	Y→C	Y→Y	
	Ethanol	Y→C	Y→Y	
	Toluene	Y→C	Y→Y	
p-Nitro phenol	Water	Y→C	Y→Y	
	Ethanol	C→C	C→Y	
	Toluene	C→C	C→Y	

C = Colorless; P = Pink; R = Red; V = Violet; Y = Yellow

the surface acidity* is < 1.2. TiO_2 -II powder was basic and the surface basicity lies above 7.2, the pK_a value of the indicator p-nitro phenol. These are quite significant results in that two TiO_2 powders having different surfaces can be differentiated readily by the indicator method. This result is the reason why one cannot use a given TiO_2 powder as representative of the oxide layer on Ti 6-4. Rather, one must make the acid-base measurements directly on the Ti 6-4 surface.

* The terms 'acid strength', 'acidity' and 'surface acidity' have been used in the literature to describe solid surfaces. However, it is important to define precisely what is meant by each of these terms. For example, the term 'acidity' may mean acid strength or the amount of acid.

The acid strength of a solid surface is usually defined by H_o functions as in equation [14]. The pK_a values are measured in solution. Therefore one has to be careful in using the pK_a values measured in solution to define the acid strength of a surface. The activity coefficient (f_{BH^+}) corrections in turn relates to that in solution rather than on the surface.

However, for the purpose of this report the definition of 'surface acidity' is taken as the acidity comparable to an aqueous solution which has a pH value close to the pK_a value of an indicator which is present in both acid and base forms in that solution. The term surface acidity defined in this way will be used henceforth. Thus, the surface acidity of TiO_2 -I is < 1.2, the pK_a value of benzeneazodiphenyl amine.

PART II: Study of Titanium 6-4 Metal Coupons with Indicators

In order to measure the acid-base properties of the Ti 6-4 surface, the color changes of indicators were determined visually and spectrophotometrically.

(A) Visible Absorption Spectra of the Indicators

The maximum wavelength of absorption (λ_{max}) in the visible spectra and the colors of the acid and base forms of the indicators used to study Ti 6-4 surfaces are tabulated in Table VII. The values are consistent with the literature values (9).

(B) Surface Pretreatments

Turco, phosphate-fluoride and Pasa-Jell are three pretreatments used in cleaning the titanium 6-4 metal surfaces prior to adhesive bonding. Physical changes of the surfaces due to the pretreatment have been examined previously (64). Scanning electron photomicrographs of phosphate-fluoride etched, Turco etched and Pasa-Jell etched titanium 6-4 metal surfaces are shown in Figures 5-7 respectively (64). It is clear that there are significant differences of the surfaces after the different pretreatments. In both the phosphate-fluoride and Pasa-Jell etched Ti 6-4 surfaces, there are well defined alpha (grey region) and beta (white region) phases present. In the Pasa-Jell etched Ti 6-4 surface, the beta phase is larger than in the phosphate-fluoride etched surface. However, the Turco etched Ti 6-4 surface is entirely different from the previous two surfaces, in that the beta phase is

TABLE VII
COLORS AND λ_{MAX} VALUES OF THE ACID AND BASE
FORMS OF THE INDICATORS

Indicator	Acid form		Base form	
	Color	$\lambda_{\text{max}} \text{ (nm)}$	Color	$\lambda_{\text{max}} \text{ (nm)}$
Benzeneazo diphenylamine	V	530	Y	390
Bromphenyl blue	Y	440	B	593
Bromcresol green	Y	445	B	615
Bromcresol purple	Y	445	B	593
Bromthymol blue	Y	450	B	615
Orange 1	O	490	V	515
Thymol blue	Y	440	B	605

B = Blue; O = Orange; V = Violet; Y = Yellow

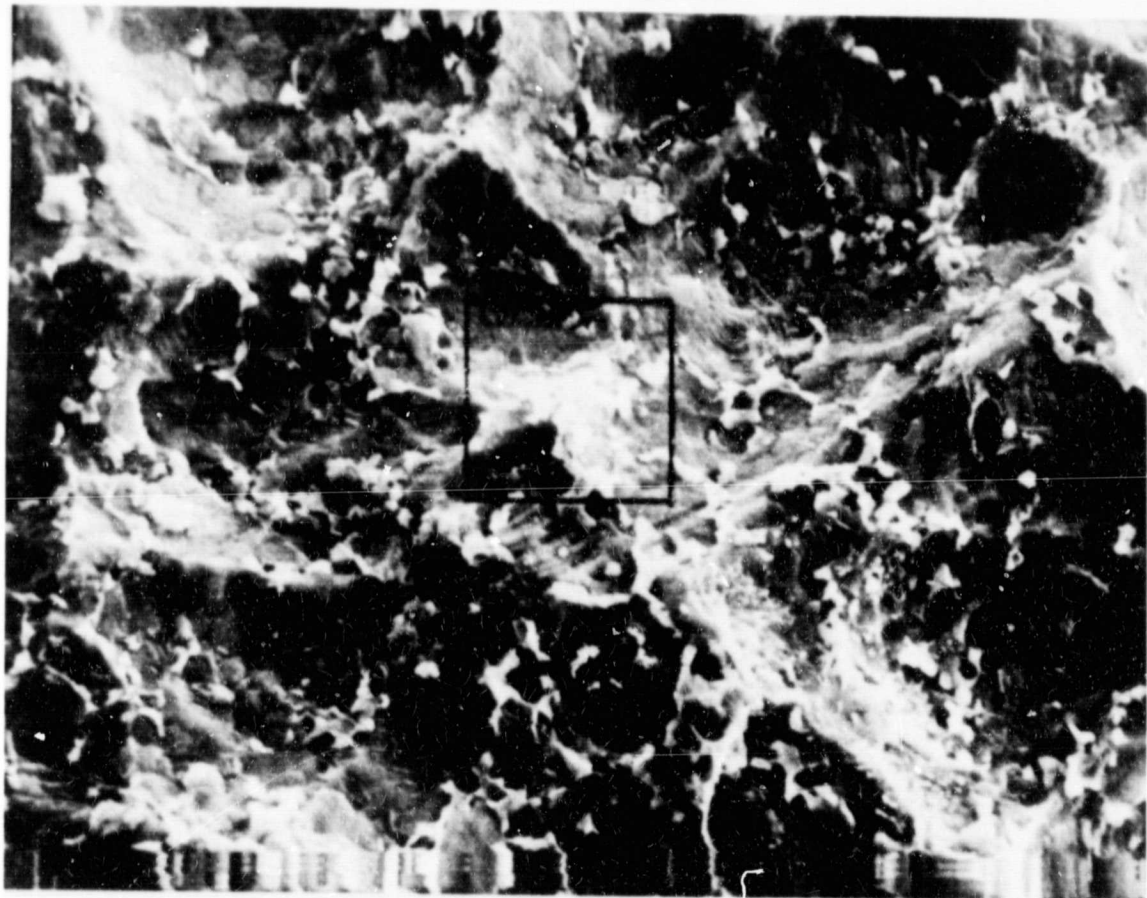


Figure 5. Scanning Electron Photomicrographs of
Phosphate-Fluoride Etched Ti 6-4 Surface

ORIGINAL PAGE IS
OF POOR QUALITY

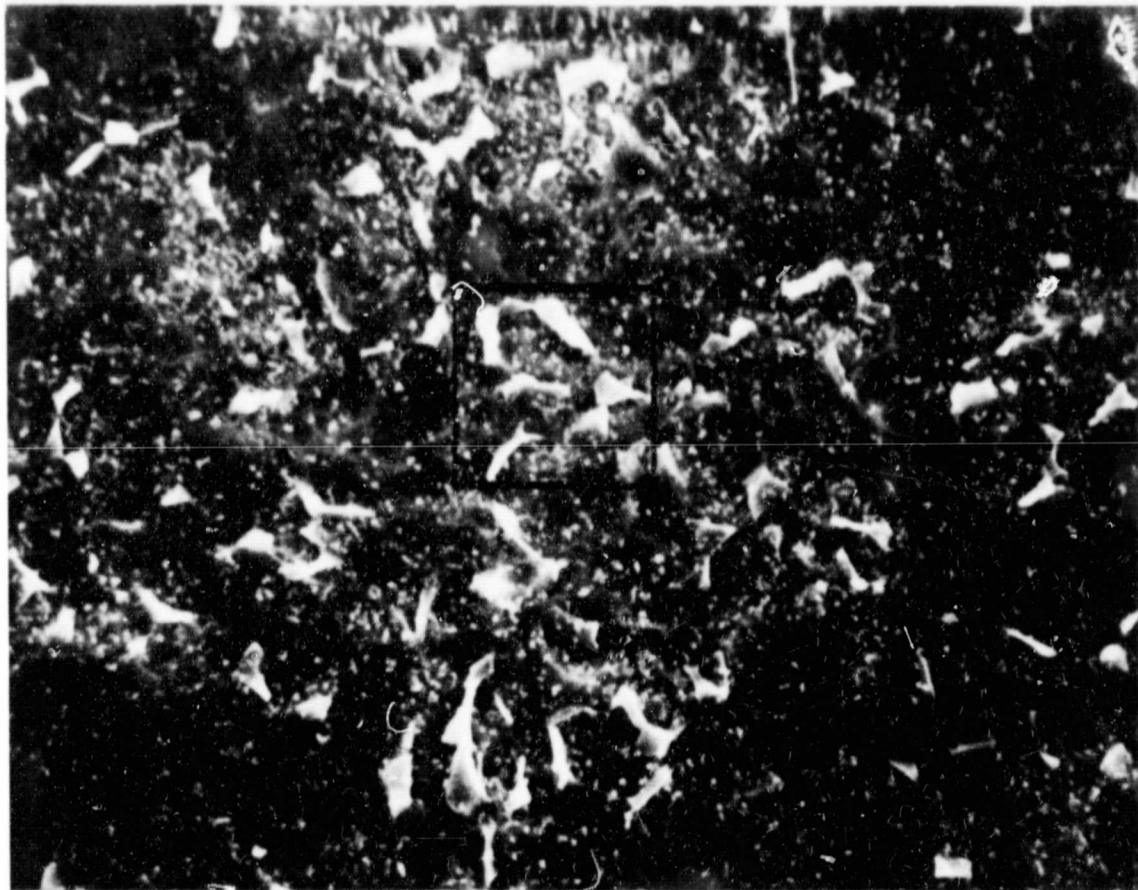


Figure 6. Scanning Electron Photomicrographs of Pasa-Jell Etched Ti 6-4 Surface

ORIGINAL PAGE IS
OF POOR QUALITY

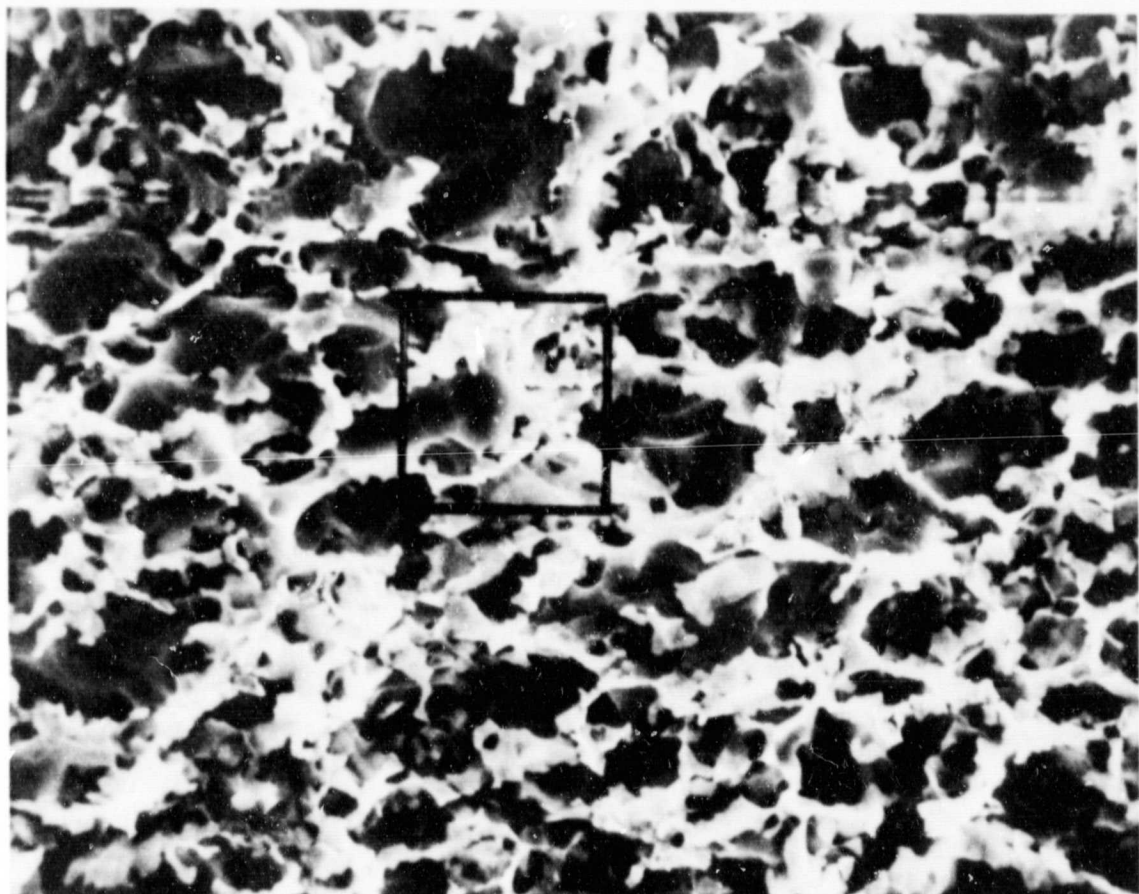


Figure 7. Scanning Electron Photomicrographs of Turco Etched Ti 6-4 Surface

predominant. It is important to examine how the chemical properties such as acidity and basicity differ for these surfaces.

Visual color changes and maximum wavelength of absorption λ_{max} in the diffuse reflectance visible spectra of the indicators on Ti 6-4 surfaces pretreated with the Turco, phosphate-fluoride and Pasa-Jell processes are given in Tables VIII, IX and X respectively. The diffuse reflectance visible spectra for bromthymol blue on phosphate-fluoride etched and Turco etched Ti 6-4 surfaces are shown in Figures 8 and 9 respectively. A broad, low intensity absorption peak centered at 464 nm was observed for bromthymol blue on phosphate-fluoride etched Ti 6-4 surface. The observed visual color changes and λ_{max} values are in good agreement with each other. Comparison of these results with the results in Table VII gives the form of the indicator present on the surface. As shown in Table VIII, the indicator thymol blue changes color from base form to its conjugate acid form on the Turco etched Ti 6-4 surface, while bromthymol blue remains in its base form. Thus the Turco etched Ti 6-4 surface is rather basic and its basicity lies between 9.2 and 7.3.

Results from Table IX indicate that the Ti 6-4 surface after the treatment with the phosphate-fluoride process is acidic and the acidity lies between 7.3, the pk_a value of indicator bromthymol blue and 4.9, the pk_a value of bromcresol green.

The Ti 6-4 surface after treatment with the Pasa-Jell process is acidic as given in Table X, and the acidity is less than or equal to 7.3 the pk_a value of the indicator bromthymol blue. The results with

TABLE VIII
 λ_{MAX} VALUES AND COLOR CHANGES OF THE INDICATORS
 ON TURCO ETCHED TITANIUM 6-4 SURFACE

Indicator	pK_a at Zero Ionic Strength	Color Changes Before Drying	Colors and λ_{max} (nm) Values after Drying
Benzeneazo diphenylamine	1.2	Y-Y	464 Y
Bromphenol blue	4.1	B-B	635; 436 (Weak) B
Bromcresol green	4.9	G-B-G	644; 460 (Weak) B-G
Bromcresol purple	6.4	B-B	620 B
Bromthymol blue	7.3	B-B	604 B
Orange 1	-	O-O	Not Detectable
Thymol blue	9.2	B-Y	476 Y

B = Blue; G = Green; O = Orange; Y = Yellow;
 B-G = Blue-Green

TABLE IX

 λ_{MAX} VALUES AND COLOR CHANGES OF THE INDICATORS
 ON PHOSPHATE-FLUORIDE ETCHED SURFACE

Indicator	pK _a at Zero Ionic Strength	Color Changes Before Drying	Colors and λ_{max} (nm) Values after Drying
Benzeneazo diphenylamine	1.2	Y-Y	436 Y
Bromphenol blue	4.1	B-B	636; 436 (Weak) B
Bromcresol green	4.9	G-B-G	616; 472 (Weak) B-G
Bromcresol purple	6.4	B-B-Y	466; 650 (Weak) Y with V spots
Bromthymol blue	7.3	B-Y-B	464 Y
Orange 1	-	O-O	408 O
Thymol blue	9.2	B-Y	478 Y

B = Blue; G = Green; O = Orange; Y = Yellow;
 B-G = Blue-Green; Y-B = Yellow-Blue; B-Y = Blue-Yellow

TABLE X
 λ_{MAX} VALUES AND COLOR CHANGES OF THE INDICATORS
 ON PASA-JELL ETCHED Ti 6-4 SURFACE

Indicator	pK _a at Zero Ionic Strength	Color Changes Before Drying	Colors and λ_{max} (nm) Values after Drying
Benzeneazo diphenylamine	1.2	Y-Y	436 Y
Bromphenol blue	4.1	B-B	620; 484 (Weak) B
Bromcresol green	4.9	G+B-G	668; 484 (Weak) B-G
Bromcresol purple	6.4	B+B-Y	476 B-Y
Bromthymol blue	7.3	B+B-Y	476; 648 (Weak) Y with B spots
Orange 1	-	O-O	500 O
Thymol blue	9.2	B-Y	436 Y

B = Blue; G = Green; O = Orange; Y = Yellow;
 B-G = Blue-Green; B-Y = Blue-Yellow

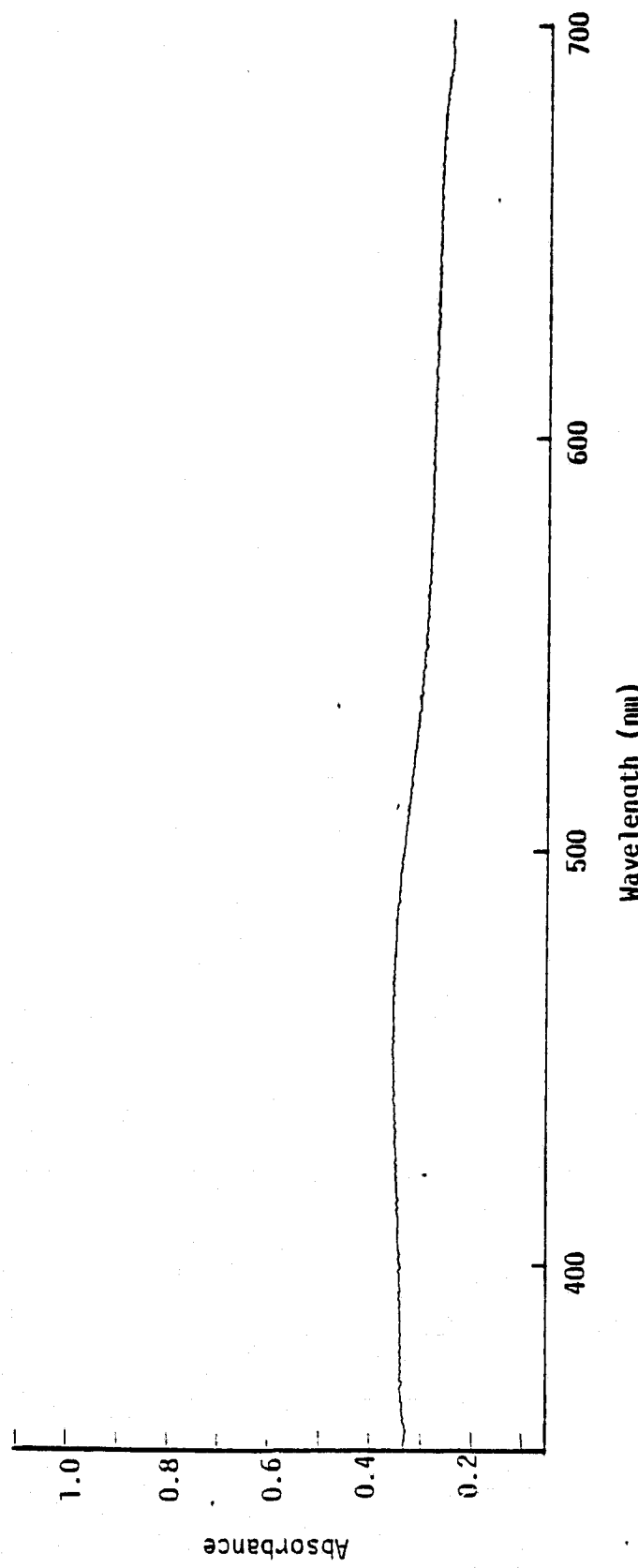


Figure 8. Diffuse Reflectance Visible Spectra of Bromthymol Blue on Phosphate Fluoride Etched Surface

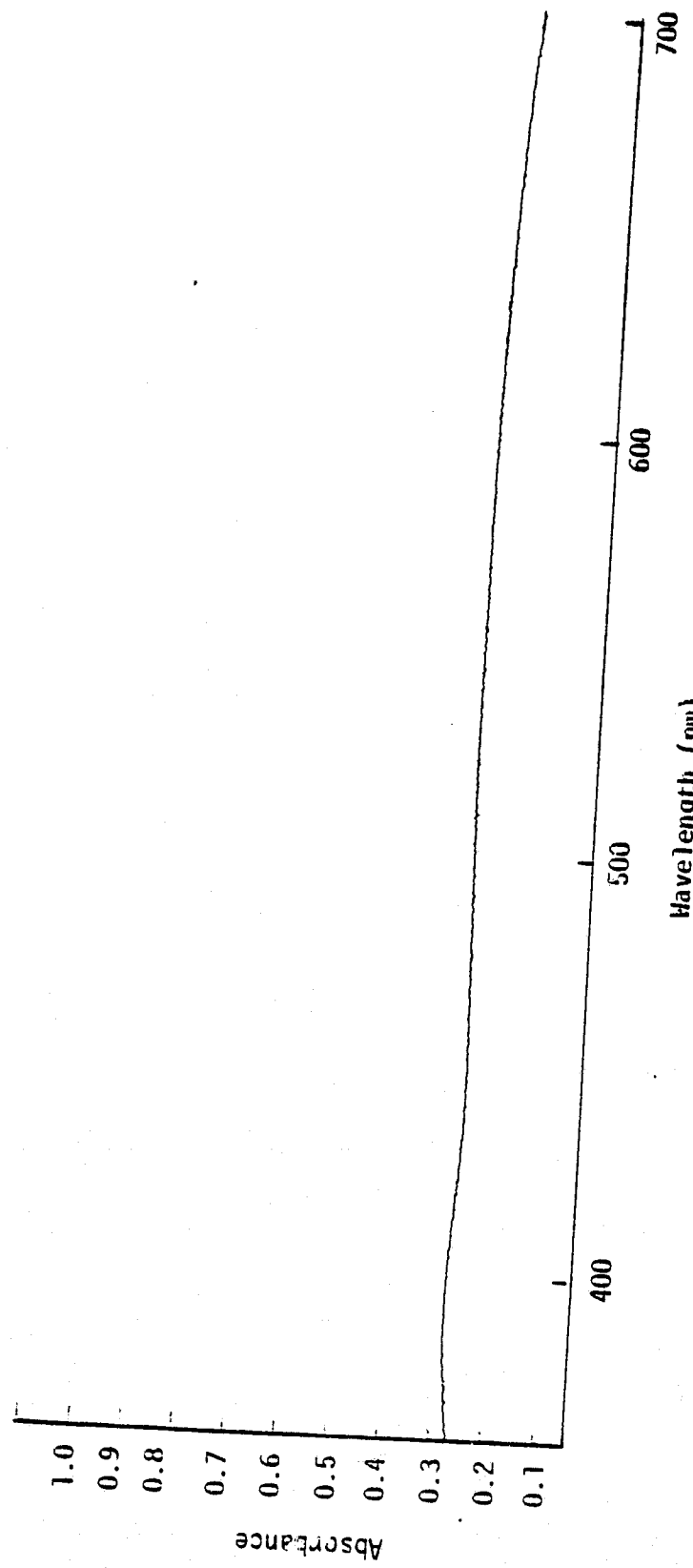


Figure 9. Diffuse Reflectance Visible Spectra of Bromthymol Blue on Turco Etched Surface

bromcresol purple were not reproducible and are not discussed further. The small peaks in the region 430-480 nm for bromcresol green and brom phenol blue on all the surfaces may be due to the acidic impurities present in the indicator.

(C) Effect of Experimental Conditions

(1) Time effects

It is suspected that surface characteristics are usually modified when a pretreated metal surface is exposed to the atmosphere. However definitive experimental results supporting such changes are scarce. It is interesting to examine how the acid-base properties change and the rate at which the changes occur when the surface is exposed to the air. The color change and λ_{max} values from diffuse reflectance visible spectra of the indicators bromthymol blue and thymol blue on Turco and phosphate-fluoride etched surfaces obtained at different time intervals after exposing to the atmosphere are given in Table XI-XIV respectively.

As shown in Table XI, the blue base form of the indicator brom thymol blue appears after 10 hours on the phosphate-fluoride etched surface. It is clear that there is a decrease in surface acidity when the phosphate-fluoride etched surface is exposed to air for 10 hours.

It is generally accepted in adhesion technology that if a freshly pretreated Ti 6-4 surface is not bonded within one hour, the surface should be primed for protection. Thus, this work establishes the surface chemistry basis for the priming process namely, to prevent changes in surface acidity leading to decreased bond strength.

TABLE XI
TIME EFFECTS ON PHOSPHATE-FLUORIDE ETCHED
Ti 6-4 SURFACE WITH BROMTHYMOL BLUE

Time (Hours)	Color changes before drying	Colors and λ_{\max} (nm) values after drying
1	B→B-Y	444 Complete Y
2	B→B-Y	440 Complete Y
5	B→B-Y	448 Mainly Y with small B spots
10	B→B-Y	400; 630 Mainly Y with B spots
25	B→B-Y	456; 652 Mainly Y with B spots
50	B→B-Y	424; 648 Y with B spots
100	B→B-Y	444; 632 Y with B spots

B = Blue; Y = Yellow

TABLE XII
TIME EFFECTS ON PHOSPHATE-FLUORIDE ETCHED
Ti 6-4 SURFACE WITH THYMOL BLUE

Time (Hours)	Color changes before drying	Colors and λ_{max} (nm) values after drying
1	B→Y	488 Y
2	B→Y	456 Y
5	B→Y	460 Y
10	B→Y	460 Y
25	B→Y	432 Y
50	B→Y	460 Y
100	B→Y	476 Y

B = Blue; Y = Yellow

TABLE XIII
TIME EFFECTS ON TURCO ETCHED Ti 6-4 SURFACE
WITH BROMTHYMOL BLUE

Time (Hours)	Color changes before drying	Colors and λ_{\max} (nm) values after drying
1	B→B	628 B
25	B→B	612 B
50	B→B	612 B
100	B→B	604 B

B = Blue

TABLE XIV
TIME EFFECTS ON TURCO ETCHED Ti 6-4 SURFACE
WITH THYMOL BLUE

Time (Hours)	Color changes before drying	Colors and λ_{\max} (nm) values after drying
1	B→Y	456 Y
2	B→Y	472 Y
10	B→Y	464 Y
25	B→Y	480 Y
50	B→Y	472 Y
100	B→Y	496 Y

B = Blue; Y = Yellow

The changes on the Turco etched Ti 6-4 surface are not pronounced with the indicators bromthymol blue and thymol blue. In the case of the phosphate-fluoride etched surface, since the surface acidity is very close to the pK_a value of bromthymol blue, small changes in surface acidity were seen. However the changes may have been observed on Turco etched surface, if an indicator with a pK_a value, in the range 7.3 and 9.2 was used.

(2) Effect of solvent

Aqueous solutions of bromcresol green, bromcresol purple and thymol blue existed in the base forms. However in ethanol solutions, the acid forms of bromcresol green and bromcresol purple and the base form of thymol blue were obtained. The colors of the indicators dissolved in ethanol are shown in Table XV. The visual color changes and λ_{max} values from the diffuse reflectance visible spectra of these indicator solutions on Turco and phosphate-fluoride etched Ti 6-4 surfaces are tabulated in Table XVI and XVII respectively. The color changes of the indicators in ethanol are consistent with the results obtained in aqueous solutions shown in Tables VIII and IX.

(3) Effect of concentration of the indicators

The color changes and λ_{max} values in the diffuse reflectance visible spectra of diluted (ten fold) aqueous solutions of bromthymol blue, thymol blue and bromcresol purple on Turco and phosphate-fluoride etched Ti 6-4 surfaces were determined. The visual color changes were similar to the results obtained at the higher concentrations. However the indicators at the lower concentration were not

TABLE XV
COLORS OF THE INDICATORS IN ETHANOL

Indicator	Color
Thymol blue	G-B
Bromcresol green	Y
Bromcresol purple	Y

G-B = Green-Blue; Y = Yellow

TABLE XVI

 λ_{MAX} VALUES AND COLOR CHANGES OF THE INDICATORS
IN ETHANOL ON TURCO ETCHED Ti 6-4 SURFACE

Indicator	Color Changes	$\lambda_{\text{max}} (\text{nm})$
Thymol Blue	G→Y	Not Detectable
Bromcresol green	Y→V-G	620; 476 (Weak)
Bromcresol purple	Y→V-G	605; 417 (Weak)

G = Green; Y = Yellow; V = Violet

TABLE XVII

 λ_{MAX} VALUES AND COLOR CHANGES OF INDICATORS IN ETHANOL
 ON PHOSPHATE-FLUORIDE ETCHED Ti 6-4 SURFACE

Indicator	Color Changes Before Drying	Colors and λ_{max} (nm) Values After Drying
Thymol blue	B→Y	470 Y
Bromcresol green	Y→G-V	606; 416 (Medium) G-V
Bromcresol purple	Y→V-G	612; 432 (Medium) V-G

B = Blue; G = Green; V = Violet; Y = Yellow

detectable by diffuse reflectance visible spectra.

(4) Temperature effects

Physical changes of Turco and phosphate-fluoride etched Ti 6-4 surfaces after thermal treatment have previously been observed (64). Scanning electron photomicrographs of these two surfaces after heating to 230°C in air are shown in Figures 10 and 11 respectively. For phosphate-fluoride etched Ti 6-4 coupons, it appears that the alpha phase has grown in the expense of the beta phase when exposed to air at 230°C for 10 hours. The results of thermal treatment are more dramatic in the case of the Turco etched surface than the phosphate-fluoride etched surface. The surface topography has collapsed into locally ordered planes and plate like structures now appear on the surface.

The acid-base properties of Ti 6-4 surfaces after the Turco and phosphate-fluoride processes and exposure to air at 230°C for 10 hours were observed using indicators and the results are given in Tables XVIII and XIX, respectively.

The appearance of yellow spots for brom thymol blue on Turco etched surface indicates that the base strength of the surface decreases on heating. Similarly, the acidity of the phosphate-fluoride etched surface decreases drastically on heating.

The results obtained after keeping the previously heated samples for an additional 90 hours in air at room temperature are shown in Table XX. The Turco etched surface appear to be basic while the phosphate-fluoride etched surface tends to decrease its acidity.

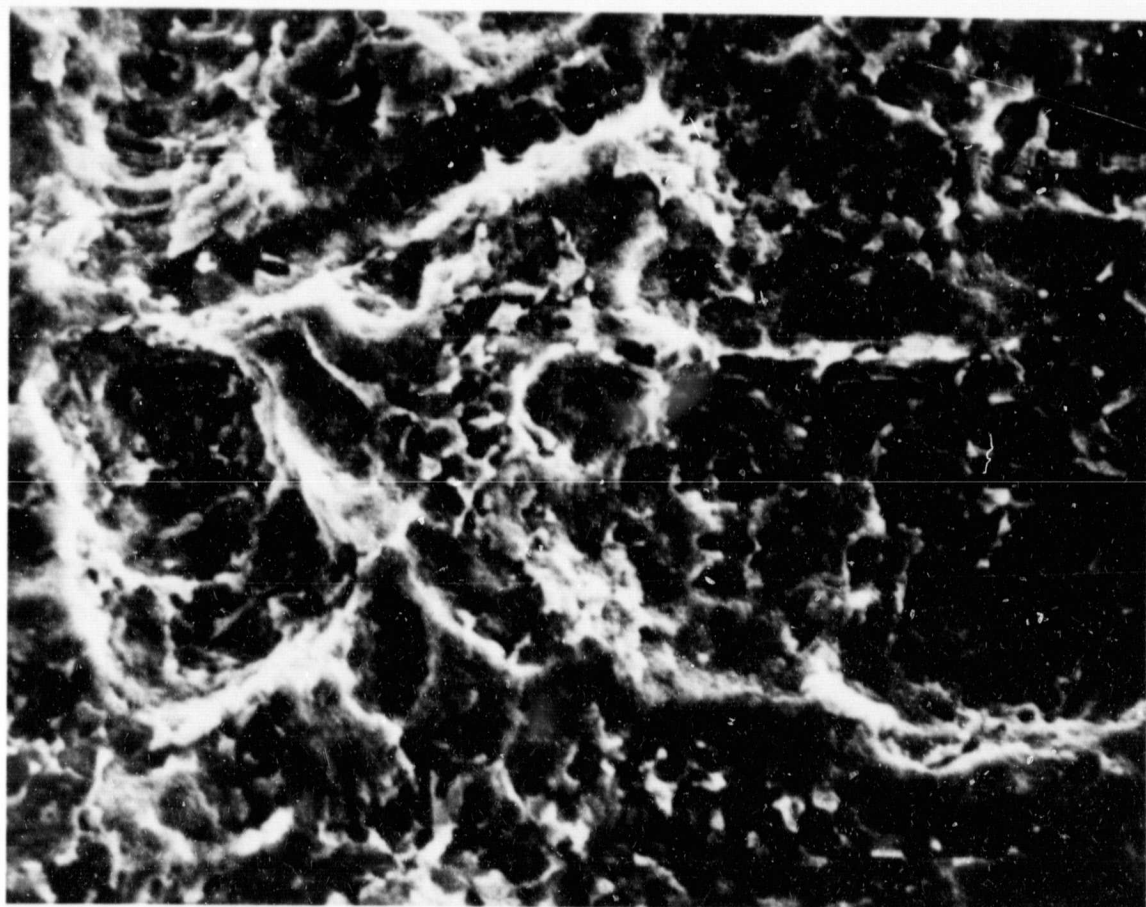


Figure 10. Scanning Electron Photomicrographs of Phosphate-Fluoride Etched Ti 6-4 Surface after Exposing to Air at 230°C for 10 Hours

ORIGINAL PAGE IS
OF POOR QUALITY

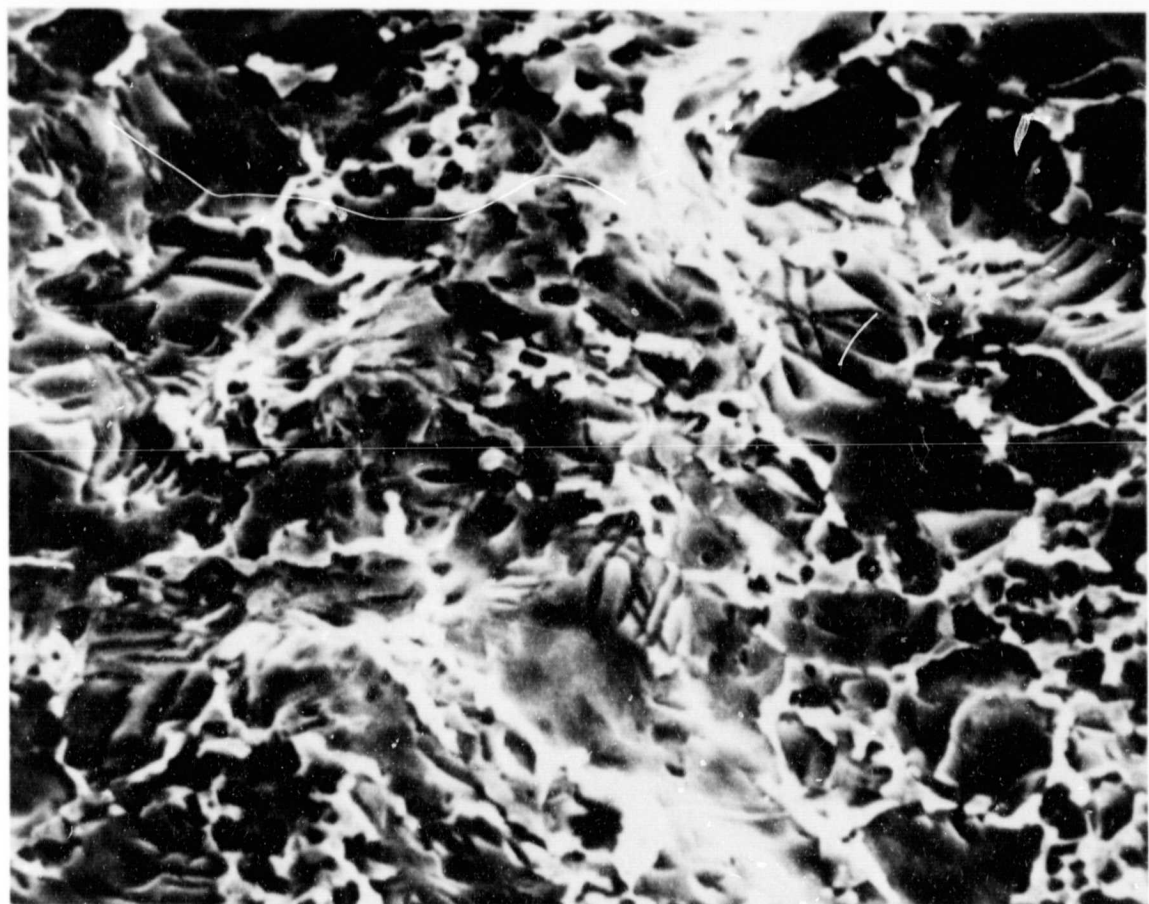


Figure 11. Scanning Electron Photomicrographs of Turco Etched Ti 6-4 Metal Surface after Exposing to Air at 230°C for 10 Hours

TABLE XVIII
TEMPERATURE EFFECTS ON TURCO ETCHED Ti 6-4 SURFACE

Indicator	Colors		λ_{\max} (nm)
	Before Drying	After Drying	
Thymol blue	B→Y	Y	456
Bromthymol blue	B→B	Mainly B with Y spots	616 (B side) 596 (Section with Y spots)

B = Blue; Y = Yellow

TABLE XIX
TEMPERATURE EFFECTS ON PHOSPHATE-FLUORIDE ETCHED
Ti 6-4 SURFACE

Indicator	Colors		λ_{\max} (nm)
	Before Drying	After Drying	
Thymol blue	B→Y	Y	448
Bromthymol blue	B→B	Mainly B with some Y spots	628

B = Blue; Y = Yellow

TABLE XX
EFFECTS OF KEEPING HEATED SAMPLES IN AIR
AT ROOM TEMPERATURE FOR 90 HOURS

Indicator	Colors		λ_{\max} (nm)	
	Before Drying	After Drying		
Pretreatment:				
Turco				
Thymol blue	B→B	Y	436	
Bromthymol blue	B→B	B	620	
Pretreatment:				
Phosphate-fluoride				
Thymol blue	B→Y	Y	452	
Bromthymol blue	B→Y-B	Y with B spots	416 648 (Weak)	

B = Blue; Y = Yellow

(5) Relative humidity effects

Color changes and λ_{\max} values of the indicators on pretreated Ti 6-4 metal coupons, placed in an environment of 100% and 0% relative humidity for the Turco and phosphate-fluoride processes are tabulated in Tables XXI and XXII respectively. In both cases, there was a problem of spreading the indicator on the surface. This may have been due to contamination of the surface by adsorption of organic materials present in the dessicators. Lindberg (65) has shown that incomplete spreading as measured by contact angles of water was a very sensitive probe of organic contamination on aluminum surfaces. Surface contamination of Ti 6-4 precludes determination of surface acidity.

(6) Effect of drying conditions

When the metals are dried in air after the pretreatments, there is a possibility of adsorbing impurities present in air thus affecting the observed color changes. The color changes and λ_{\max} values of the indicators on Turco and phosphate-fluoride etched surfaces, after drying in argon are given in Tables XXIII and XXIV respectively. In all cases, there is efficient spreading of the indicator on the surface indicating minimal contamination. It is also seen that the acidity of the phosphate-fluoride etched surface is slightly decreased in argon drying. In air drying, there is a possibility of adsorbing acidic impurities like CO_2 . However there appears to be no problem with air drying the Ti 6-4 samples for this range of surface acidities.

TABLE XXI
RELATIVE HUMIDITY EFFECTS ON TURCO ETCHED
Ti 6-4 SURFACE

Indicator	Colors		λ_{\max} (nm)
	Before Drying	After Drying	
100% Relative humidity			
Thymol blue	B→Y	Y	444
Bromthymol blue	B→B	B	640
0% Relative humidity			
Thymol blue	B→Y	Y	472
Bromthymol blue	B→B	B	604

B = Blue; Y = Yellow

TABLE XXII
RELATIVE HUMIDITY EFFECTS ON PHOSPHATE-FLUORIDE
ETCHED Ti 6-4 SURFACE

Indicator	Colors		$\lambda_{\text{max}} \text{ (nm)}$
	Before Drying	After Drying	
100% Relative humidity			
Thymol blue	B→Y	Y	436
Bromthymol blue	B→B	B	612
0% Relative humidity			
Thymol blue	B→Y	Y	476
Bromthymol blue	B→B	B	600

B = Blue; Y = Yellow

TABLE XXIII
EFFECT OF ARGON DRYING ON TURCO ETCHED
Ti 6-4 SURFACE

Indicator	Colors		λ_{\max} (nm)
	Before Drying	After Drying	
Thymol blue	B+Y	Y	484
Bromthymol blue	B+B	B	652

B = Blue; Y = Yellow

TABLE XXIV
EFFECT OF ARGON DRYING ON PHOSPHATE-FLUORIDE
ETCHED Ti 6-4 SURFACE

Indicator	Colors		λ_{\max} (nm)
	Before Drying	After Drying	
Thymol blue	B-Y	Y	464
Bromthymol blue	B-Y-B	Y with B spots	624-B portion 628; 408-Y portion

B = Blue; Y = Yellow

PART III: Electron Spectroscopy for Chemical Analysis

ESCA analysis was done to determine if shifts in binding energy were observed for the acid and base forms of the indicators.

(A) Bare Ti 6-4 Metal Coupons after Pretreatments

The results of the ESCA analysis of Ti 6-4 surfaces after phosphate-fluoride and Turco pretreatments are listed in Table XXV as reported by Chen et al. (66). Fluorine, aluminum and vanadium are present on both surfaces and trace amounts of potassium, chlorine and phosphorous are present on phosphate-fluoride pretreated Ti 6-4 surface.

The ESCA spectra of bare Ti 6-4 metal coupons after the phosphate-fluoride and Turco pretreatments were obtained. The photopeaks of C 1s, Ti 2p and O 1s for the phosphate-fluoride etched surface and C 1s, Ti 2p, O 1s and Na 1s for the Turco etched surface are shown in Figure 12 and 13 respectively. The results of the ESCA analysis are shown in Table XXVI. The indicator molecules contain both sulfur and bromine. However, neither the S 2p nor Br 3p photo peaks were detected on the Ti 6-4 surfaces before application of the indicator solutions. Both Ti 6-4 surfaces had a photopeak at 453.0 ev which was assigned to Ti 2P_{3/2} (0). The 5.2 ev separation between the Ti 2P_{3/2} (IV) and Ti 2P_{3/2} (0) photopeaks is consistent with published value (67). The phosphate-fluoride etched surface has a larger Ti (0) signal than the Turco etched surface. This clearly shows the presence of a thicker oxide layer on the Turco etched surface.

TABLE XXV
ESCA PEAK PARAMETERS FOR Ti 6-4 BEFORE AND AFTER
CHEMICAL SURFACE TREATMENTS (66)

Peak Assignment	As-received		Phosphate-Fluoride		Turco	
	BE	%	BE	%	BE	%
F 1S	684.2	2	684.2	3	685.0	2
Cr 2p _{3/2}	-	-	-	-	-	-
O 1S	530.0	24	529.5	41	529.5	32
V 2p _{3/2}	514.2	1	515.5	1	515.7	1
Ti 2p _{3/2}	457.9	6	457.0	17	457.9	10
N 1S	-	-	-	-	-	-
Ca 2p _{3/2}	346.6	1	-	-	-	-
K 2p	-	-	287.9	1	-	-
C 1S	(284.0)	59	(284.0)	35	(284.0)	53
Cl 2p	-	-	197.3	1	-	-
P 2p _{3/2}	-	-	132.6	1	-	-
Al 2S	188.5	8	118.2	1	119.1	2
Si 2p	-	-	-	-	-	-

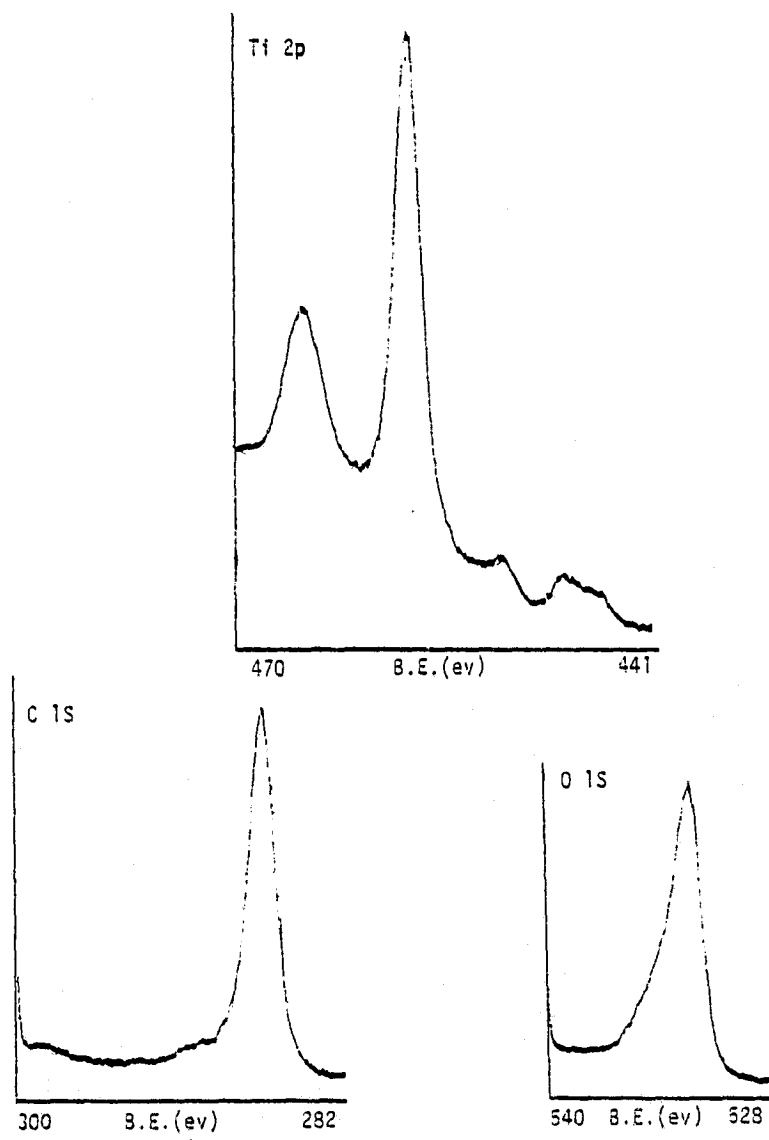


Figure 12. ESCA Photopeaks of Ti 6-4 Surface after Phosphate-Fluoride Pretreatment

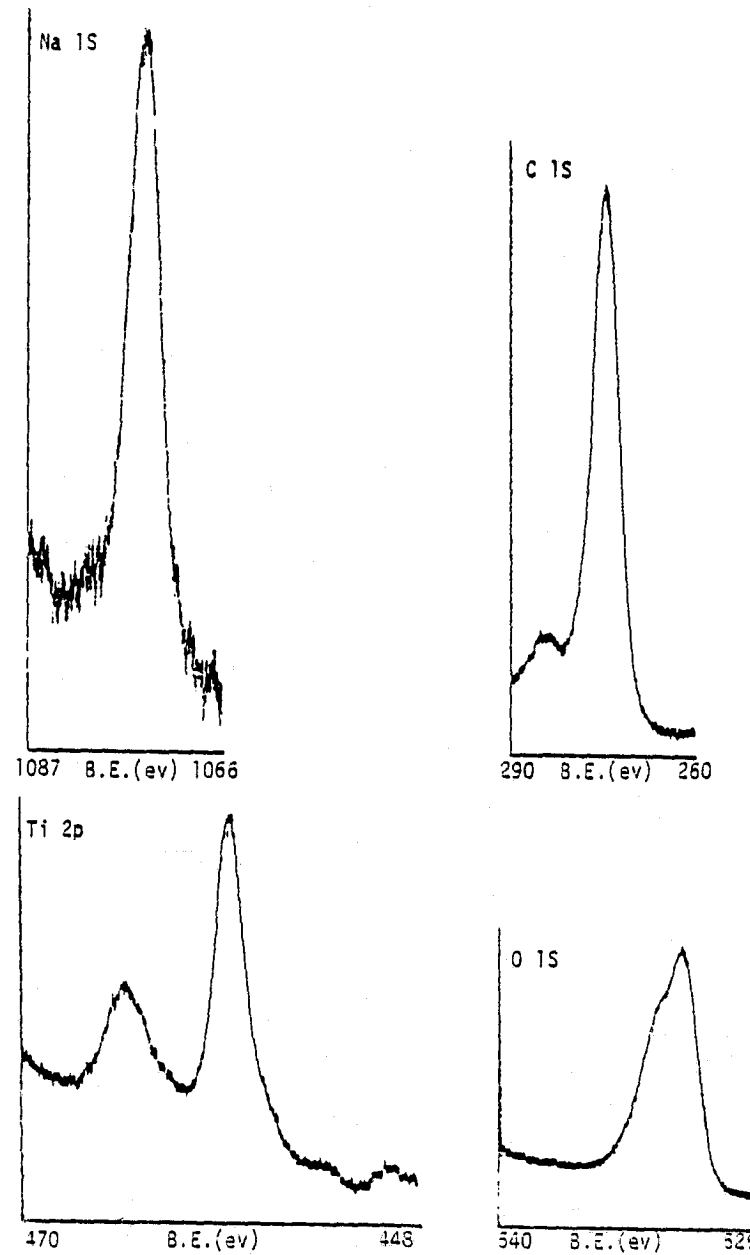


Figure 13. ESCA Photopeaks of Ti 6-4 Surface after Turco Pretreatment

TABLE XVI
RESULTS OF THE ESCA ANALYSIS OF BARE Ti 6-4
SURFACE AFTER TURCO AND PHOSPHATE-FLUORIDE PRETREATMENTS

Element	Turco		Phosphate Fluoride	
	Binding Energy (ev)	Atomic Fraction	Binding Energy (ev)	Atomic Fraction
C 1S	284.6	0.645	284.6	0.340
Na 1S	1071.2	0.059		
Ti 2p _{1/2} (IV)	464.1		464.4	
Ti 2p _{3/2} (IV)	458.2	0.092	458.6	0.075
Ti 2p _{3/2} (0)	453.0	0.002	453.4	0.005
O 1S			0.203 (Total) (1)530.5 (2)532.2 (3)High B.E. Small Side quantity	0.239 (Total) Ratio: (1)/(2)=1.312 (2)High B.E. Small Side quantity

The oxygen peak for the Turco etched surface was asymmetric and was resolved into two components as shown in Figure 14. The main peak at the lower binding energy of 530.5 ev is due to the lattice oxygen. The peak at 532.2 ev may be due to the adsorbed oxygen (68). The small amount of oxygen observed at the highest binding energy may be due to the surface contamination by an oxy-containing organic compound. The presence of a small photopeak on the high binding energy side of the C 1s photopeak is further evidence for this type of contamination where source is unknown.

(B) Bromthymol Blue Indicator Spread on the Pretreated Ti 6-4 Metal Coupons

The results obtained from the ESCA spectra after spreading bromthymol blue on the Turco etched and phosphate-fluoride etched Ti 6-4 surfaces and bromthymol blue indicator with HCl, on Ti 6-4 surfaces are shown in Table XXVII.

From the diffuse reflectance visible spectra, it was found that the base form of bromthymol blue is present on the Turco etched Ti 6-4 surface. As shown in Table XXVII, two O 1s photopeaks at binding energies of 530.6 ev and 532.4 ev were obtained when the bromthymol blue was present on the Turco etched Ti 6-4 surface. The ratio of intensity of the O 1s photopeak at 530.6 ev to the O 1s photopeak at 532.2 ev is greater for bromothymol blue on the Turco etched sample than for the bare Turco etched Ti 6-4 metal as shown on comparing the results in Tables XXVI and XXVII. Thus the major

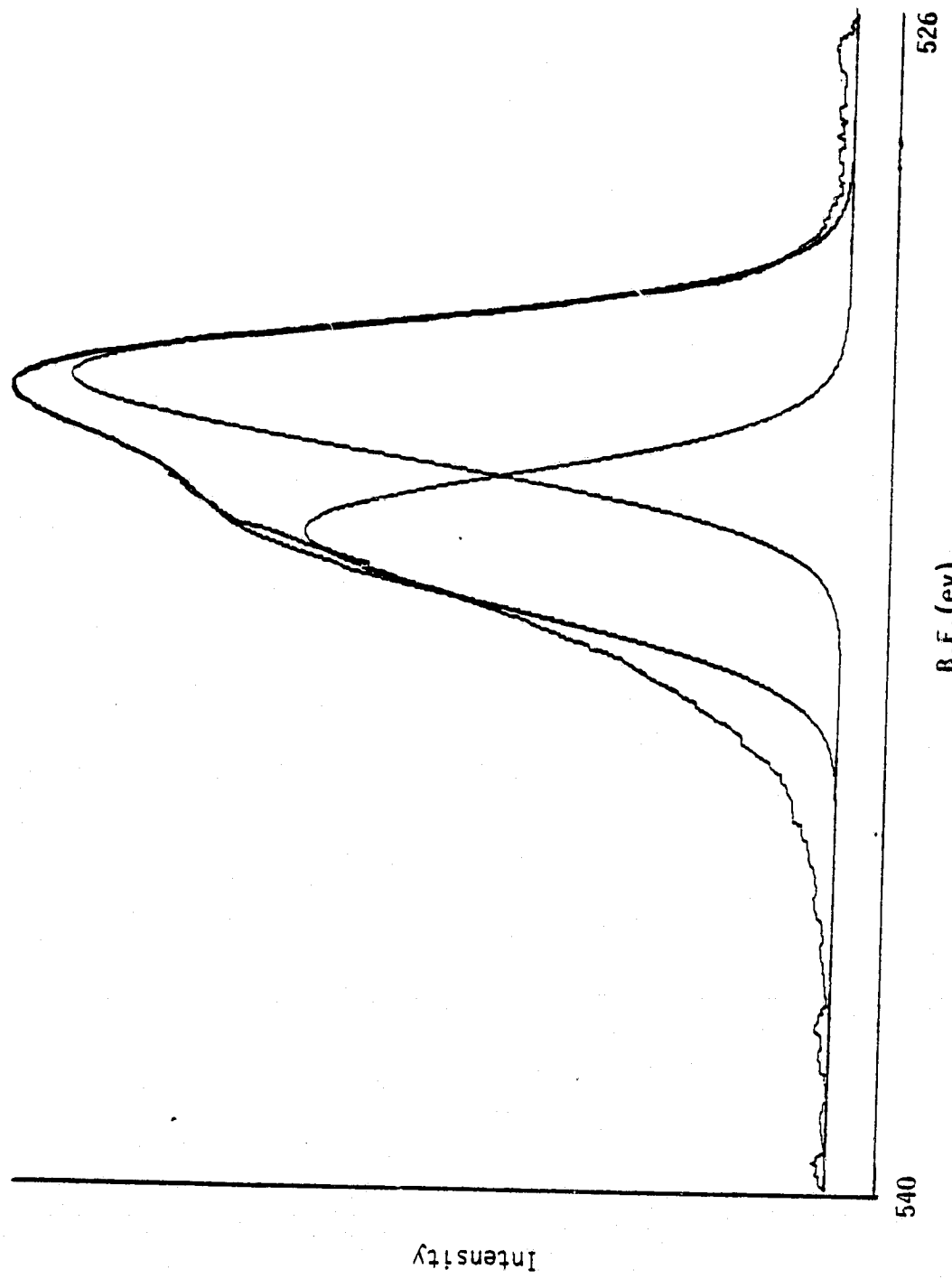


Figure 14. Oxygen 1s Photopeak after Resolving into Two Components on Turco Etched Ti 6-4 Surface

TABLE XXVII

RESULTS OF THE ESCA ANALYSIS, AFTER SPREADING THE BROMTHYMOL BLUE ON
PHOSPHATE-FLUORIDE ETCHED AND TURCO ETCHED Ti 6-4 SURFACES AND BROMTHYMOL BLUE
WITH HCl ON THE Ti 6-4 SURFACE

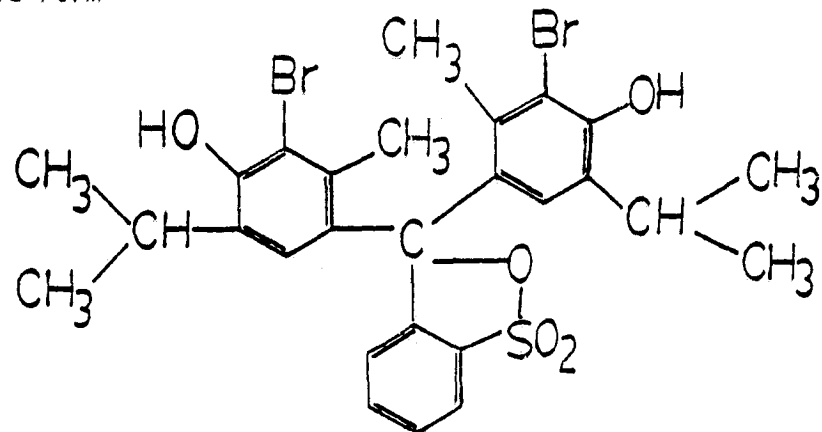
Element	Turco		Phosphate-Fluoride		Bromthymol Blue + HCl	
	Binding Energy (ev)	Atomic Fraction	Binding Energy (ev)	Atomic Fraction	Binding Energy (ev)	Atomic Fraction
C 1S	284.6	0.594	284.6	0.679	284.6	0.680
S 2p _{3/2}	168.0	0.022	167.8	0.035	168.0	0.044
Br 3p _{3/2}	183.7	0.014	183.5	0.015	183.6	0.037
Na 1S	1071.7	0.037	1071.7	0.049	1071.6	0.005
Ti 2p _{1/2}	464.3	--	464.2	--	464.8	--
2p _{3/2}	458.4	0.052	458.2	0.011	458.7	0.011
O 1S	(1)530.5 (2)532.4 (3)533.6	0.2(Total) Ratio: (1)/(2)=1.76 Ratio: (2)/(3)=2.57	531.5	0.206	532.1	0.214

peak at binding energy of 530.6 ev is characteristic of oxygen for the bromthymol blue on the Turco etched surface. There is a marked difference of 1.5 ev between this binding energy and the binding energy of oxygen for the bromthymol blue with HCl.

The structures of the base and the acid forms of the bromthymol blue are shown in Figure 15. It is clear that there are two different kinds of oxygen in the acid and base forms of the indicator. The oxygen being more negative in the base form is expected to have a lower binding energy than the acid form. Thus the difference in binding energies of oxygen for the base form present on the Turco etched surface and the acid form present in the sample containing bromthymol blue and HCl is consistent with results based on the different structural formulas.

From the diffuse reflectance spectra, it was concluded that the acid form of bromthymol blue is present on the phosphate-fluoride etched surface. As shown in Tables XXVII and XXVI there is a difference in binding energies of oxygen for bromthymol blue on the phosphate-fluoride etched surface and the bare phosphate-fluoride etched surface. Thus it is clear that the binding energy of 531.5 ev is characteristic of the oxygen of bromthymol blue on the phosphate-fluoride etched surface. It is also seen in Table XXVII, that the binding energy of oxygen for bromthymol blue on the phosphate-fluoride etched surface is very close to the value of oxygen in bromthymol blue with HCl, but 1.0 ev different from the value of oxygen for bromthymol blue on the Turco etched surface. Since the acid form

(A) Acid Form



(B) Base Form

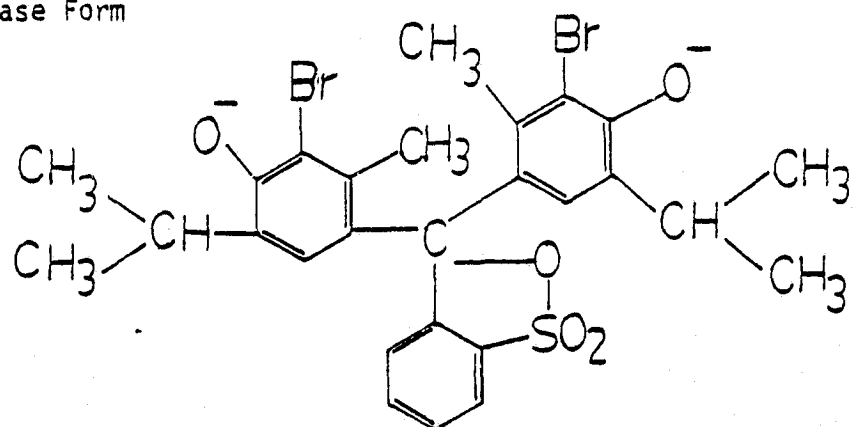


Figure 15. The Structures of Acid and Base Forms
of Bromthymol Blue

of the indicator is present on the phosphate-fluoride etched surface, this is consistent with the results expected from the structural formulas. The above results indicate that the acid and base forms of the indicators having different structures can be monitored using the ESCA technique.

(C) Pretreated Metal Coupons Immersed in the Bromthymol Blue Solution

The ESCA results of the Turco etched and phosphate-fluoride etched surfaces after immersion in the bromthymol blue solution are shown in Table XXVIII. As shown in Table XXVI, the bare metals after both treatments, do not show the presence of sulfur and bromine. Thus the presence of sulfur and bromine, after immersing the two surfaces in bromthymol blue solution, indicates that there is adsorption of the indicator onto the pretreated surfaces. Greater adsorption occurs on the phosphate-fluoride etched surface as noted by the greater atomic fraction of sulfur. It is also seen that the O 1s photopeak at 532.2 ev, which was originally present on the Turco etched surface, has decreased appreciably after immersion in bromthymol blue solution.

(D) Pretreated Metal Coupons Immersed in the Thymol Blue Solution

Results of the ESCA analysis, after immersion of the Turco and phosphate-fluoride etched Ti 6-4 surfaces in thymol blue solution are shown in Table XXIX. The presence of sulfur on both samples, indicates again that there is adsorption of the indicator onto the etched

TABLE XXVIII
RESULTS OF THE ESCA ANALYSIS OF TURCO ETCHED AND
PHOSPHATE-FLUORIDE ETCHED Ti 6-4 SURFACES AFTER
IMMERSING IN BROMTHYMOL BLUE SOLUTION

Element	Turco Etched Surface		Phosphate-Fluoride Etched Surface	
	Binding energy (ev)	Atomic Fraction	Binding energy (ev)	Atomic Fraction
C 1S	284.6	0.400	284.6	0.360
S 2p _{3/2}	167.9	0.006	168.2	0.012
Br 3p _{3/2}	182.8	0.004	183.6	0.004
Na 1S	1071.3	0.035	1071.5	0.041
Ti 2p _{1/2} (IV) 2p _{3/2} (IV)	463.9 458.0	0.103	464.1 458.2	0.104
O 1S	529.6	0.452	530.0	0.468

C - 2

TABLE XXIX
RESULTS OF THE ESCA ANALYSIS OF TURCO ETCHED AND
PHOSPHATE-FLUORIDE ETCHED Ti 6-4 SURFACES AFTER
IMMERSING IN THYMOL BLUE SOLUTION

Element	Turco Etched Surface		Phosphate-Fluoride Etched Surface	
	Binding energy (ev)	Atomic Fraction	Binding energy (ev)	Atomic Fraction
C 1S	284.6	0.707	284.6	0.549
S 2p _{3/2}	168.1	0.010	168.1	0.014
Na 1S	1071.5	0.061	1071.7	0.014
Ti 2p _{1/2} (IV)	464.0		464.2	
Ti 2p _{3/2} (IV)	458.2	0.157	458.4	0.076
O 1S	529.9	0.640	530.2	0.327

surfaces. Greater adsorption occurs on the phosphate-fluoride etched surface as noted by greater atomic ratio of $[S]/[Ti]$. After immersion in the thymol blue solution the amount of oxygen at 532.2 ev, which was originally present on the Turco etched sample, is appreciably decreased. This result is not clear but consistent with what was observed in bromthymol blue solution. The adsorbed oxygen may have dissolved in the indicator solution during the immersion process.

It has been shown above that the acid and base forms of the indicators having different structures can be monitored using the ESCA technique.

PART IV: Specular Reflectance Infra-Red Spectra

Differences in surface acidity of Ti 6-4 should lead to differences in the amount of stearic acid adsorbed from cyclohexane solution. A basic surface would be expected to adsorb more stearic acid than an acidic surface. Specular reflectance infra-red spectroscopy (SRIRS) was used to monitor stearic acid adsorption on Ti 6-4.

Major peaks and their assignments from the specular reflectance infra-red spectra of stearic acid deposited from cyclohexane solution on Ti 6-4 metal coupons are tabulated in Table XXX. Previous work by Honeycutt and Wightman (69) showed that intensities of peaks in the specular reflectance infra-red spectra of silicone on Al and KRS-5 surfaces are directly proportional to the amount present on the surface. Thus the intensities of infra-red peaks are used to discuss the amount of stearic acid adsorbed on Ti 6-4 coupons after immersion in the cyclohexane solutions of stearic acid.

Intensities of the major peaks in the specular reflectance infra-red spectra of bare Ti 6-4 metal coupons after pretreatment with the Turco and phosphate-fluoride processes are given in Table XXXI. The broad peak in the region of $1080\text{-}1390\text{ cm}^{-1}$ is assigned as the stretching vibration of the Ti-O bond. This peak is broader and more intense in the case of the phosphate-fluoride etched surface than for the Turco etched surface.

Peak intensities after immersing the etched surfaces in stearic acid solutions with concentrations 0.001%, 0.01% and 0.02% by weight

TABLE XXX

MAJOR PEAKS IN THE SPECULAR REFLECTANCE INFRA-RED SPECTRA OF
STEARIC ACID ON TITANIUM 6-4 METAL COUPONS

Wave Number (cm ⁻¹)	Peak Assignments
2920	C-H stretching of CH ₃ and CH ₂
2850	
1700	C=O stretching
1465	C-H deformation of CH ₃ or CH ₂
1300	C-H deformation of long chain hydrocarbon
940	O-H bending in acids
720	Rocking of CH in a long chain hydrocarbon

TABLE XXXI
INTENSITIES OF THE PEAKS IN THE SPECULAR REFLECTANCE
INFRA-RED SPECTRA OF PRE-TREATED Ti 6-4 METAL COUPONS

Wave Number (cm^{-1})	Turco Scale Expansion	Intensities	Wave Number (cm^{-1})	Phosphate-Fluoride Scale Expansion	Intensities
1130-1250	x10	13 Broad	1080-1390	x10	20 Broad

are given in Table XXXII. The results indicate that there is more stearic acid adsorbed on the Turco etched surface than on the phosphate-fluoride etched surface for all the concentrations. This difference was especially noted in the intensities of the 2920 cm^{-1} and 1700 cm^{-1} peaks for the 0.02% concentration. For better comparison, some of the major specular reflectance infra-red peaks of stearic acid adsorbed from the 0.02% solution on pretreated surfaces are shown in Figures 16 and 17. The infra-red results are consistent with the results obtained by the indicator method. That is, the Turco etched Ti 6-4 surface being more basic than the phosphate-fluoride etched surface adsorbed more stearic acid.

Specular reflectance infra-red spectroscopy can be used in the study of surface acidity. However, the results of SRIRS give only a relative measure of surface acidity whereas the indicator method gives a quantitative measure.

TABLE XXXII
INTENSITIES OF THE PEAKS IN THE SPECULAR REFLECTANCE
INFRA-RED SPECTRA OF PRE-TREATED Ti 6-4 METAL COUPONS
AFTER IMMERSING IN 0.001%, 0.01%, and 0.02%
STEARIC ACID SOLUTIONS

		Turco		Phosphate-Fluoride			
		Wave Number (cm^{-1})	Scale Expansion	Intensities	Wave Number (cm^{-1})	Scale Expansion	Intensities
(A) 0.001%	Conc.						
		x10	x10	12.5	2360	x10	All the peaks
		x10	x10	25.0	1720	x10	were very
		x10	x10	17.0	1700	x10	narrow and
		x10	x10	15.0	1670	x10	difficult to
					1309-1080	x10	distinguish
							from noise
							20(Broad)
(B) 0.01%	Conc.						
		x10	x10	23	2360	x10	Very
		x10	x10	23	1700	x10	Narrow
		x10	x10	24	1690	x10	peaks
					1250-1090	x10	24(Broad)

TABLE XXXII (continued)

(C) 0.02% Conc.	Turco			Phosphate-Fluoride		
	Wave Number (cm^{-1})	Scale Expansion	Intensities	Wave Number (cm^{-1})	Scale Expansion	Intensities
2920	x10		77	2920	x10	
2860	x10		55	2860	x10	
2360	x10		15	2360	x10	
1700	x5		60	1700	x10	35 Very
1460	x10		43	1690	x10	31 Narrow
1300	x10		49	1540	x10	38 Peaks
940	x10		16	1520	x10	39
720	x10		53	1309-1009	x10	36
						21 (Broad)

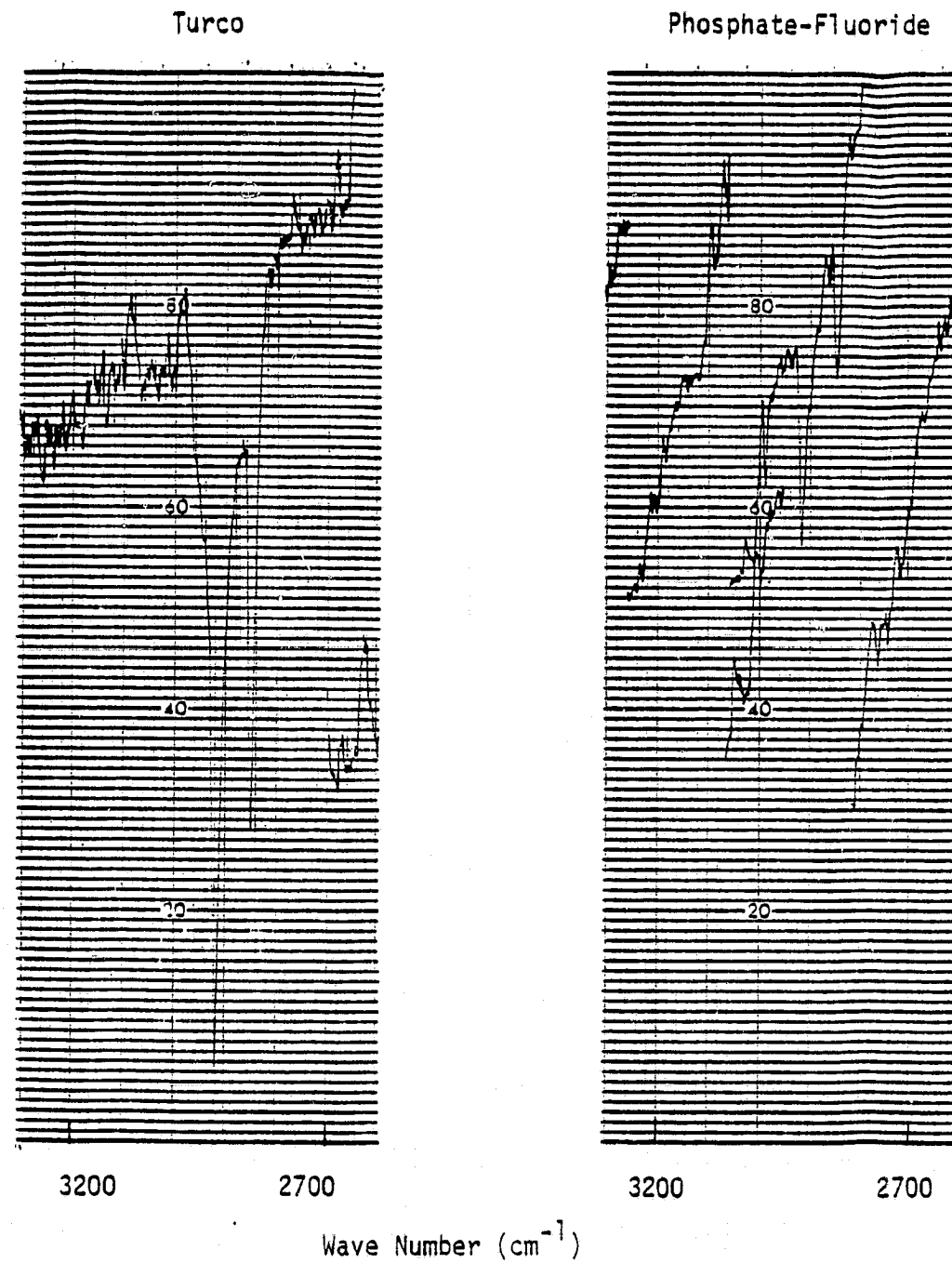


Figure 16. Specular Reflectance, Infra-Red Peaks in the Region $2700\text{-}3200\text{ cm}^{-1}$ of Stearic Acid Adsorbed on Ti 6-4 Surfaces

ORIGINAL PAGE IS
OF POOR QUALITY

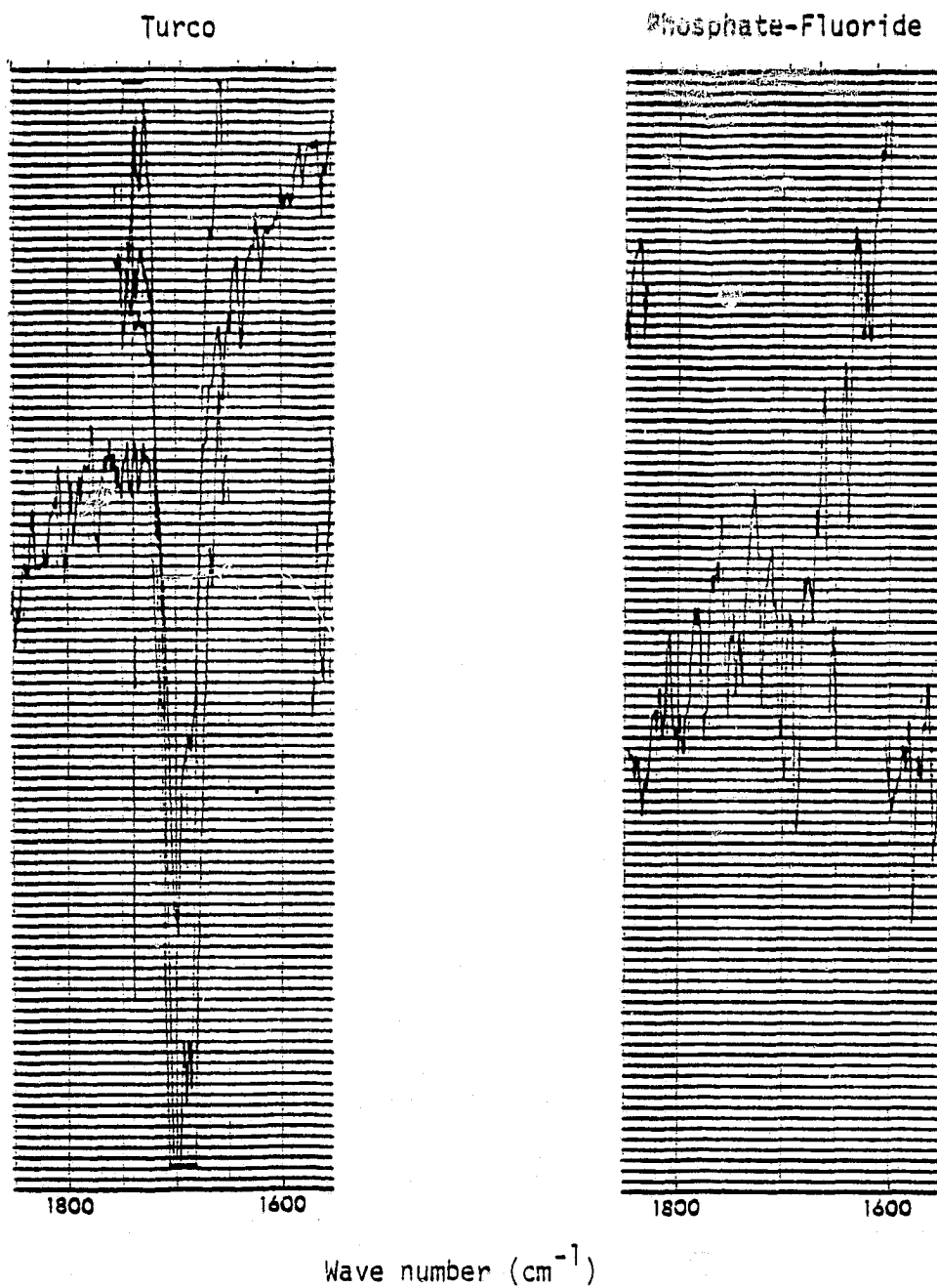


Figure 17. Specular Reflectance Infra-Red Peaks in the Region $1600\text{-}1800\text{ cm}^{-1}$, of 0.02% Stearic Acid Adsorbed on Pretreated Ti 6-4 Surfaces

PART V: A Model for the Ti 6-4 Surface

A model for the Ti 6-4 surface can be deduced to account for the surface acidity based on all the results described above. It is important to note that both Lewis and Bronsted sites can interact with the indicators to change the color (4). Thus the Bronsted and Lewis sites cannot be differentiated by indicator method.

For the phosphate-fluoride etched surface, photopeaks characteristic of both Ti (IV) and Ti (0) were observed with ESCA. Thus the surface of the phosphate-fluoride etched Ti 6-4 consists of a thin oxide layer (<5 nm) as shown in Figure 18. This surface was found to be acidic by the indicator method. The Bronsted acid sites may be due to the hydroxyl groups as shown in Figure 18 (4). The phosphate-fluoride treatment involved the reaction with HF (aq) and indeed F 1S photopeaks were observed with ESCA (66). The Bronsted acidity may also be due to the functional groups shown in Figure 19 (4). The acidity of the OH groups may be due to the weakening of the OH bond by the inductive effect of the highly electronegative fluorine.

Lewis acid sites may also be present on the surface as coordinately unsaturated cations. These cations may also be hydrated to form Bronsted acid sites as shown in Figure 20. The acidity may also result due to the formation of Ti-OH_2^+ by acid treatment as shown in Figure 21 (70).

When the phosphate-fluoride etched surface was exposed to air, a decrease in acidity was observed after 10 hours. This may have

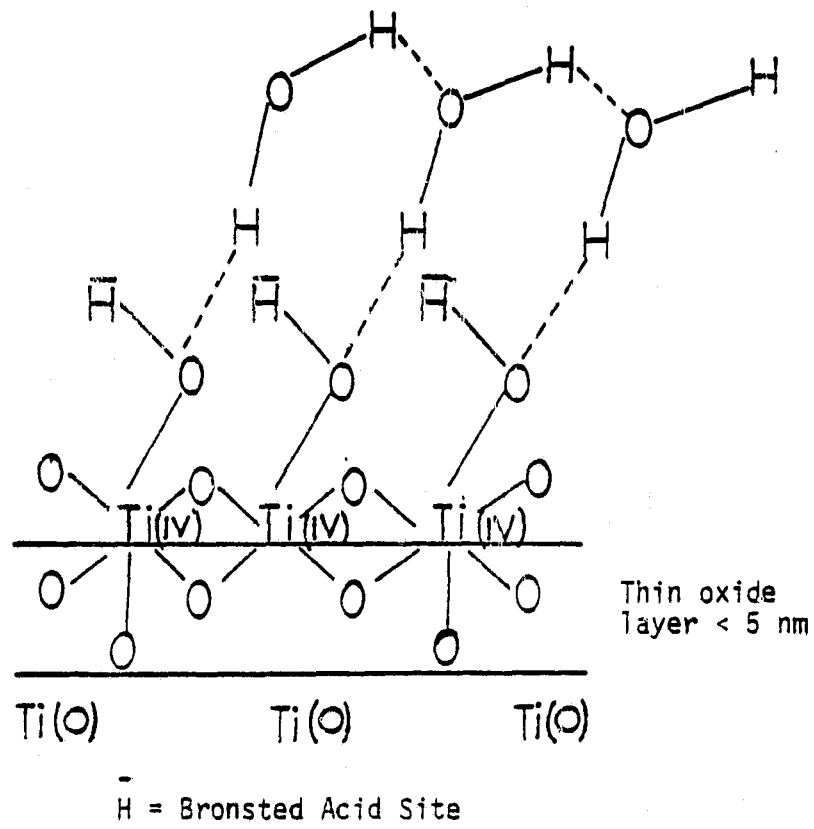


Figure 18. Acid Sites on Ti 6-4 Surface after Phosphate-Fluoride Pretreatment

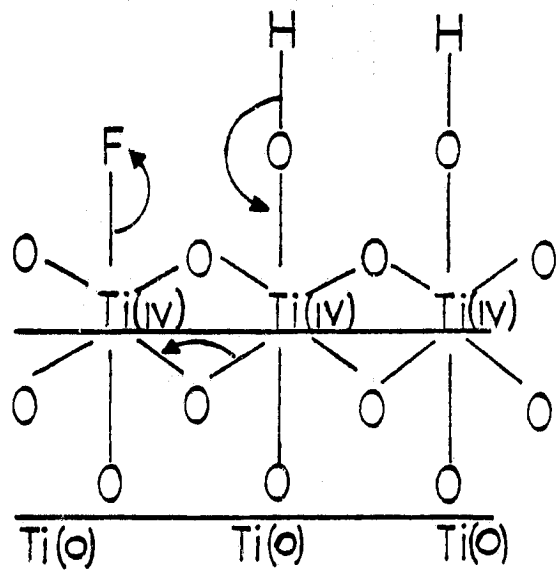


Figure 19. Acid Sites on Ti 6-4 Surface after Phosphate-Fluoride Pretreatment

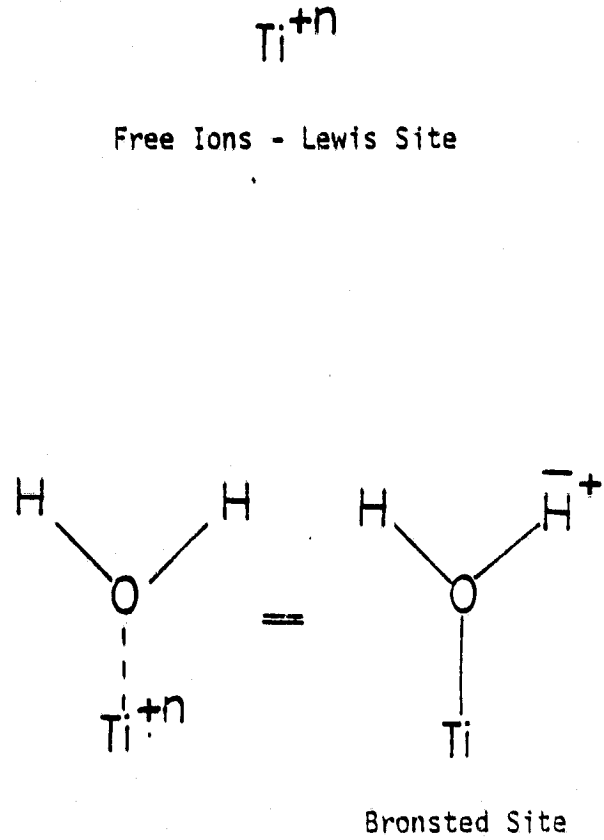


Figure 20. Acid Sites on Ti 6-4 Surface after Phosphate-Fluoride Pretreatment

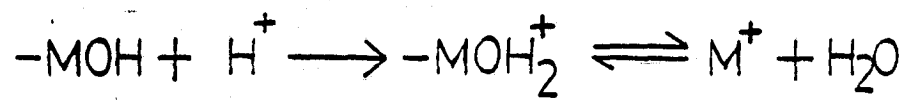
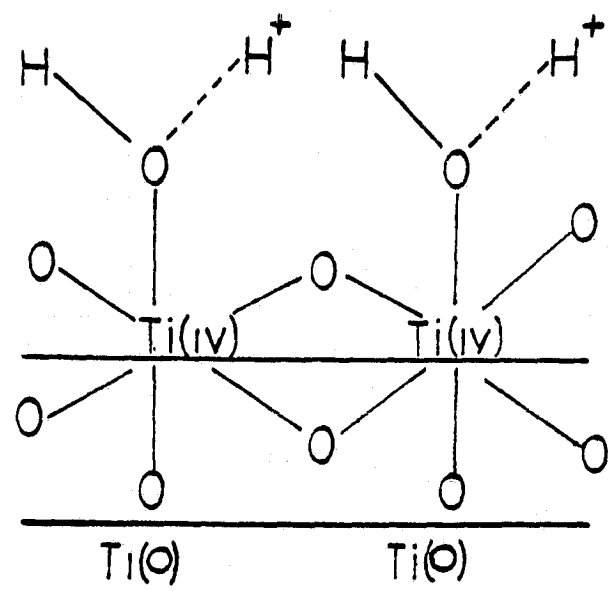
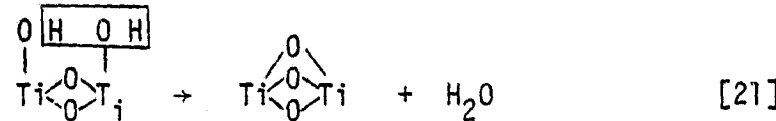


Figure 21. Acid Sites on Ti 6-4 Surface after Phosphate-Fluoride Pretreatment

been due to the oxidation of Lewis acid sites or adsorption of trace amount of organic or basic impurities like NH_3 from the laboratory environment.

When the treated metal was heated to 230°C , the acidity decreased drastically. Removal of water and condensation of adjacent hydroxyl groups as shown in reaction 21 can take place at a higher temperature (71).



Thus if Bronsted acid sites are present on the surface as shown in Figure 18 and 19, they may be removed at a higher temperature. When the heated metal samples were placed at room temperature for another 90 hours, drastic reduction of acidity was not observed. Thus the reaction which was responsible for the decrease in acidity at high temperature, has to be reversible at room temperature over a 90 hour period.

For the Turco etched surface, the ESCA results showed the presence of a small $\text{Ti}(0)$ signal. This indicates the presence of a thicker oxide layer on the Turco etched surface as shown in Figure 22. In contrast to the phosphate-fluoride etched surface, the Turco etched surface was basic to bromthymol blue. Previous work by Basila et al. (72) showed that the alkali metals completely eliminate the Bronsted acidity of silica-alumina catalysts. Since the Turco treatment involves sodium hydroxide, the elimination of acid sites on the Turco etched surface may have been due to the presence of sodium. The formation of -O^-

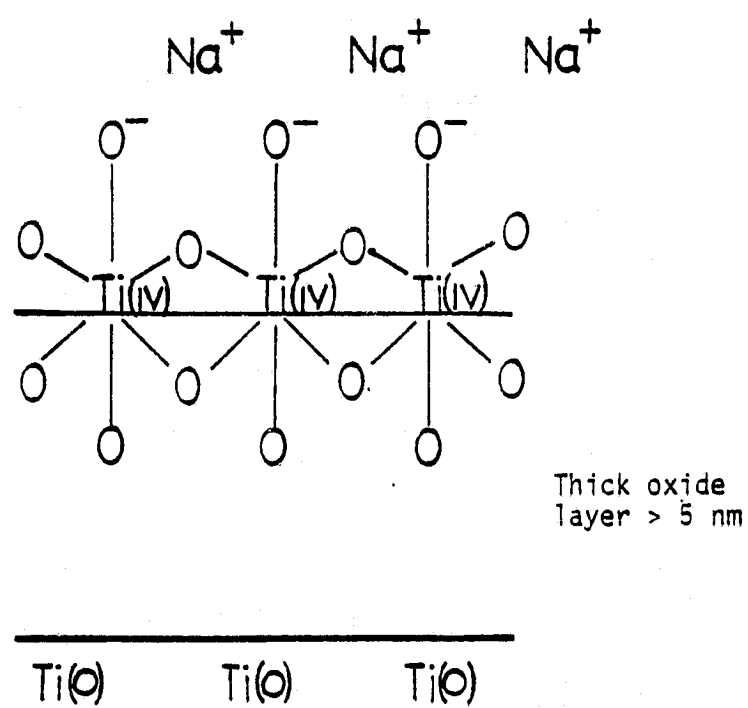
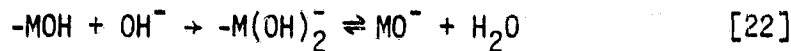


Figure 22. Functional Groups on Turco Etched
Ti 6-4 Surface

centers on the Ti 6-4 surface is possible (70) in the alkaline treatment according to the reaction



The $-\text{O}^-$ centers may be the basic centers on the Turco etched surface as shown in Figure 22 (4). When the etched metal was heated, the reduction of basicity or increase in acidity was observed. This could be due to the formation of co-ordinately unsaturated cationic Lewis acid sites at a higher temperature (70,71). When the heated metal was placed at room temperature for 90 hours, the reduction of basicity was not observed. Thus the reaction which occurred at higher temperature is reversible at room temperature over a 90 hour period.

Chapter V

CONCLUSIONS

The following conclusions were derived from a spectroscopic characterization study of the surface acidity of Ti 6-4 metal surfaces:

1. The TiO_2 powders having different surfaces can be readily differentiated by the indicator method. The solid powders $Mg(ClO_4)_2$ and TiO_2 -I were found to be acidic and the surface acidity < 1.2 . The TiO_2 -II powder was basic and the surface basicity > 7.2 .

2. The indicator method and diffuse reflectance spectroscopic measurements can be used to differentiate the acid-base characteristics of Ti 6-4 surfaces after different pretreatments. The Turco etched Ti 6-4 surface was basic and the basicity lies between 7.3 and 9.2. The phosphate-fluoride etched Ti 6-4 surface was acidic and acidity lies between 5.4 and 7.3. Ti 6-4 surface after the Pasa-Jell pretreatment was acidic and the surface acidity was ≤ 7.3 .

3. An apparent decrease in acidity was found with bromthymol blue when the phosphate-fluoride etched Ti 6-4 surface was exposed to air for 10 hours. Time effects were not observed with bromthymol blue or thymol blue on the Turco etched Ti 6-4 surface.

4. Surface acidities established using aqueous solutions of the indicators and the ethanol solutions of the indicators were in good agreement.

5. Visual color changes of the diluted (10 fold) indicator solutions on etched surfaces were in good agreement with that of

concentrated solutions. However, the color changes with diluted solutions could not be detected directly by diffuse reflectance visible spectroscopy.

6. When the pretreated Ti 6-4 metals were heated to 230°C, a decrease in basicity was observed on the Turco etched Ti 6-4 surface and a drastic decrease in acidity was observed on phosphate-fluoride etched Ti 6-4 surface, using bromthymol blue. When the heated metals were placed in air at room temperature for 90 hours, the decrease in basicity was not observed on the Turco etched Ti 6-4 surface while a slight decrease in acidity was observed on the phosphate-fluoride etched Ti 6-4 surface.

7. Binding energies of oxygen for bromthymol blue on Turco and phosphate-fluoride etched Ti 6-4 surfaces were different as detected by the ESCA technique. Thus the acid and base forms of the indicators having different structures can be monitored by ESCA technique.

8. More stearic acid was adsorbed on the Turco etched Ti 6-4 surface than on the phosphate-fluoride etched Ti 6-4 surface as detected by specular reflectance infra-red spectroscopy. This result is consistent with the greater basicity of the Turco etched Ti 6-4 as determined by the indicator method.

REFERENCES

1. Shoemaker, R. H.; Titanium Sci. Technol. 1973, 4, 2401.
2. Drago, R. S.; Vogel, G. C.; Needham, T. E.; J. Am. Chem. Soc. 1971, 93, 6014.
3. Fonkes, F. M.; Organic Coatings and Plastic Chemistry Preprints, 1979, 40.
4. Tanabe, K. "Solid Acids and Bases"; Academic Press, Inc.: New York, 1970.
5. Anderson, R. B.; Ed. "Experimental Methods in Catalytic Research", Academic Press, Inc.: New York, 1968.
6. Bell, R. P. "The Protons in Chemistry", 2nd ed., Cornell University Press: New York, 1973, Chap. 2.
7. Morrison, S. R. "The Chemical Physics of Surfaces"; Plenum Press: New York, 1977, Chap. 1.
8. Bishop, E.; Ed. "Indicators"; Pergamon Press: Oxford, 1972.
9. Kolthoff, I. M.; Rosenblum, C.; "Acid-Base Indicators"; MacMillan Inc.: New York, 1937.
10. Walling, C.; J. Am. Chem. Soc., 1950, 72, 1164.
11. Weil-Malherbe, H.; Weiss, J.; J. Am. Chem. Soc., 1948, 2164.
12. Brown, B. F.; Fujii, C. T.; Dahlberg, E. P.; Electro Chemical Society, 1969, 116, 218.
13. Telichkun, V. P.; Tarasevich, Y.; Goncharuk, V. V.; Theor. Eksp. Khim., 1977, 13, 131; Chem. Abstr. 1977, 86, 177840a.
14. March, J. "Advanced Organic Chemistry", 2nd ed.; McGraw Hill Inc: New York, 1970.
15. Hammett, L. P.; Deyrup, A. J.; J. Am. Chem. Soc., 1932, 54, 2721.
16. Hammett, L. P. "Physical Organic Chemistry", 2nd Ed; McGraw Hill, Inc: New York, 1970.
17. Yamanaka, T.; Tanabe, K.; J. Phys. Chem., 1976, 80, 1723.
18. Holm, V. C. F.; Bailey, G. C.; Clark, A.; J. Phys. Chem., 1959, 60, 29.

19. Affrossman, A.; Mitchell, G. W.; Mitchell, G. J.; J. Catal., 1975, 38, 516-17.
20. Klanig, W.; J. Phys. Chem., 1976, 80, 262-9.
21. Walvekar, S. P.; Halgeri, A. B.; Indian J. Chem., 1973, 11, 662-5.
22. Johnson, O.; J. Phys. Chem., 1955, 59, 827.
23. Take, J.; Kawai, H.; Yoneda, Y.; Bull. Chem. Soc. Jap., 1977, 46, 3568-9.
24. Take, J.; Kawai, H.; Yoneda, Y.; Bull. Chem. Soc. Jap., 1977, 50, 2428-31.
25. Yamanaka, T.; Tanabe, K.; J. Phys. Chem., 1975, 79, 2409-11.
26. Matsumara, Y.; Hagiwara, S.; Takahashi, H.; Carbon, 1976, 14 163-7.
27. Kubouva, Y.; J. Phys. Chem., 1963, 67, 769.
28. Ballou, E. V.; Barth, R. T.; Flinn, R. A.; J. Phys. Chem., 1961, 65, 1639.
29. Malinowski, S.; Szezpanska, S.; Sloczynski, J.; J. Catalysis, 1967, 7, 68.
30. Larson, J. G.; Hall, W. K.; J. Phys. Chem., 1965, 69, 3080.
31. Basila, M. R.; J. Phys. Chem., 1962, 66, 2223.
32. Poncelet, G.; Dubru, M. L.; J. Catalysis, 1978, 52, 321.
33. Defosse, D.; Canesson, P.; J. Chem. Soc. Faraday Trans. 1, 1976, 72, 2565.
34. Knoezinger, H.; Krietenbrink, H.; Ratnasamy, P.; J. Catalysis, 1977, 48, 436.
35. Dewing, J.; Monks, G. T.; Youll, B.; J. Catalysis, 1977, 48, 440-1.
36. Scokart, P. O.; Declerck, F. D.; Semples, R. E.; Roxhet, P. G.; J. Chem. Soc. Faraday Trans. 1, 1977, 73, 359.

37. Hair, M. L.; Hertl, W.; J. Phys. Chem., 1970, 74, 91.
38. Kupcha, L. A.; Kravchuk, L. S.; Markevich, S. V.; Potapovich, A. K.; Kinet. Katal., 1976, 17, 1081, Chem. Abstr. 1977, 86, 9039c.
39. Defosse, C.; Canesson, P.; Rouxhet, P. G.; Delmon, B.; J. Catalysis, 1978, 51, 269.
40. Takimoto, K.; Miura, M.; Bull. Chem. Soc. Jap., 1971, 44, 1534.
41. Galkin, V. P.; Golubev, V. B.; Lunina, E. Va.; Zh. Fiz. Khim., 1974, 48, 1747-50, Chem. Abstr., 1975, 82, 35341g.
42. Hendra, P. J.; Turner, I. D. M.; Loader, E. J.; Stacey, M.; J. Phys. Chem., 1974, 78, 300.
43. Gay, I. D.; Liang, S.; J. Catalysis, 1976, 44, 306.
44. Stone, F. S.; Zecchina, A.; Proc. Int. Congr. Catal., 1976, (Pub. 1977), 1, 162.
45. Adams, J. B.; J. Geo. Phys. Res., 1974, 79, 4826.
46. Sato, H.; Yasuniwa, T.; Bull. Chem. Soc. Jap., 1974, 47, 368.
47. Weakley, T. J. R.; J. Chem. Soc., Dalton Trans., 1973, 3, 341.
48. Matsunago, Y.; Saito, G.; Bull. Chem. Soc. Jap., 1972, 45, 963-4.
49. Tandon, S. P.; Govil, R. C.; Spectrosc. Lett., 1972, 5, 81.
50. Hecht, H. G.; Mod. Aspects of Reflectance Spectros. Proc. Symp., Chicago, 1967, Penum Press.
51. Joyner, R. W.; Surface Science, 1977, 63, 291.
52. Joyner, R. W.; Roberts, M. W.; Proc. Roy. Soc. London, Ser. A., 1976, 350, 107.
53. Clarke, T. A.; Gay, I. D.; Law, B.; Mason, R.; Faraday Discuss. Chem. Soc., 1976, 60, 119.
54. Anderson, A. B.; Hoffman, R.; J. Chem. Phys., 1974, 61, 4545.
55. Roberts, R. F.; J. Electron Spectrosc. Relat. Phenom., 1974, 4, 273.

56. Bordass, W. T.; Linett, J. W.; Nature, 1969, 222, 660.
57. Hollaway, P. H.; Madey, T. E.; Campbell, C. T.; Rye, R. R.; Houston, J. E.; Surface Sci. 1979, 88, 121.
58. Pireaux, J. J.; Ghijsen, J.; McGowan, J. W.; Verbist, R.; Surface Sci., 1979, 80, 488.
59. Ito, M.; Suetaka, W.; Surface Sci. 1977, 62, 308.
60. Higashiyama, T.; Takenaka, T.; J. Phys. Chem., 1974, 78, 941.
61. Wan, C. Z.; Haller, G. L.; J. Phys. Chem., 1979, 83, 1154.
62. Wagner, C. D.; et al. "Handbook of X-ray Photoelectron Spectroscopy", 1st ed.: Perkin Elmer: Eden Prairie, Minn. 1979.
63. Scofield, J. H.; J. Electron Spectrosc. and Related Phenomena, 1976, 8, 129.
64. Chen, W.; Dwight, D. W.; Wightman, J. P.; A Fundamental Approach to Adhesion, NASA Report, 1978.
65. Smith, T.; Lindberg, G.; Surface Technology, 1979, 9, 1-29.
66. Chen, W.; Dwight, D. W.; Kiang, W. R.; Wightman, J. P.; "Surface Contamination Genesis, Detection and Control", 2, Plenum Press, New York, 1979 (Ed. Mittal, K. L.)
67. Carlson, T. A. "Photoelectron and Auger Spectroscopy", Plenum Press, New York, 1975, 358.
68. Anderson, S. L. T.; J. Chem. Soc. Faraday Trans. I, 1979, 75, 1356.
69. Hohencutt, R. H.; Wightman, J. P.; J. Vac. Sci. Technol., 1977, 14, 742.
70. Parks, G. A.; Chem. Rev., 1965, 65, 177.
71. Parfitt, G. D.; Urwin, D.; Wiseman, T. J.; J. Colloid and Interface Sci., 1971, 36, 217.
72. Basila, M. R.; Kantner, T. R.; Rhee, K. H.; J. Phys. Chem., 1964, 68, 3197.

APPENDIX I
THREE PRETREATMENT PROCESSES FOR THE Ti 6-4 METAL COUPONS

APPENDIX I

THREE PRETREATMENT PROCESSES FOR THE Ti 6-4 METAL COUPONS

(A) Turco 5578 Method for Cleaning Ti 6-4 Panels

1. Solvent wipe- methylethyl ketone
2. Alkaline clean-immerser in Turco 5578,37.6 g/l, 70-80°C
for 5 minutes.
3. Rinse-deionized water at room temperature
4. Etch-immerser in Turco-5578,419 g/l, 80-100°C for
10 minutes
5. Rinse-deionized water at room temperature
6. Rinse-deionized water at 60-70°C for 2 minutes
7. Dry-air at room temperature.

(B) Pasa-Jell 107 Method for Cleaning Ti 6-4 Panels

1. Solvent wipe-methylethyl ketone
2. Alkaline clean-immerser in Sprex AN-9,30.1 g/l, 80°C
for 5 minutes
3. Rinse-deionized water at room temperature
4. Pickle-immerser for 5 minutes at room temperature in solution
containing 15 g nitric acid 15% by weight; 3 g hydrofluoric acid
3% by weight; and 82 g deionized water
5. Rinse-deionized water at room temperature
6. Pasa-Jell 107 paste-apply to titanium surface with an acid
resistant brush covering the entire surface by cross brushing
7. Dry-for 20 minutes

8. Rinse-deionized water at room temperature.
9. Dry-air at room temperature.

(C) Phosphite/Fluoride Method for Cleaning Ti 6-4 Panels

1. Solvent wipe-methylethyl ketone
2. Alkaline clean-immerser in Sprex AN-9,30.1 g/l, 80°C for 15 minutes
3. Rinse-deionized water at room temperature
4. Pickle-immerser for 2 minutes at room temperature in solution containing 350 g/l of 70% nitric acid and 31 g/l of 48% hydrofluoric acid
5. Rinse-deionized water at room temperature
6. Phosphate/fluoride treatment-Soak for 2 minutes at room temperature in solution containing 50.3 g/l of tri sodium phosphate; 20.5 g/l of potassium fluoride; and 20.1 g/l of 48% hydrofluoric acid
7. Rinse-deionized water at room temperature
8. Hot water soak-deionized water at 65°C for 15 minutes
9. Final rinse-deionized water at room temperature
10. Dry-air at room temperature.

APPENDIX II
POLYMER SYNTHESIS SUMMARY

At NASA Langley Research Center, experimental work was conducted on the synthesis, characterization, and evaluation of the following materials as high temperature and/or high performance structural resins.

1. Acetylene-terminated phenylquinoxaline oligomers
2. Acetylene-terminated imide oligomers
3. Poly-N-alkylenebenzimidazoles
4. Cyanate-terminated polysulfones

In addition, basic work was performed to determine the nature of the product from the thermally induced reaction of an ethynyl substituted imide model compound.

Consultation was provided in the following areas.

1. Improved structural resins for conventional use (rubber toughened epoxides, cyanates, 350° F cure epoxies)
2. Quality control of epoxy prepreg
3. High temperature structural resins

During this reporting period, two papers were presented. The titles and abstracts are given below.

"Thermal Reaction of N-(3-Ethynylphenyl)phthalimide" P. M. Hergenrother, G. E. Sykes and P. R. Young, 178th National ACS Meeting, Div. of Petroleum Chem. Preprints 24(1), 243 (1979).

Polymers from the thermally induced chain extension of acetylene-terminated imide oligomers exhibit promise for use as high temperature structural materials. As a guide to polymer formation, the thermally induced reaction of an acetylenic model compound,

N-(3-ethynylphenyl) phthalimide (EPPI), was studied using differential scanning calorimetry, high pressure liquid chromatography, infrared and mass spectroscopy. It was of interest to determine the minimum temperature to initiate reaction of the ethynyl group, the effect of longer time and higher temperature upon the product and the identity of the major components in the product. Although the exact structures were not determined, two dimers, three trimers and a tetramer were found to be the principal minor components from the thermally induced reaction of EPPI and higher molecular weight materials (oligomeric) were identified as the major components.

"Status of High Temperature Laminating Resins and Adhesives",
P. M. Hergenrother and N. J. Johnston, 178th National ACS Meeting,
Div. Org. Coatings and Plastics Chem. Preprints 40, 460 (1979).

During the last twenty years, a major effort has been devoted to the development of polymers for use as functional and structural resins in high temperature environments. In spite of this effort and the demand for these materials primarily in the electrical and aerospace industries, only a few thermally stable polymers are commercially available. This is due primarily to an unfavorable combination of price, processability, and performance inherent in all of the high temperature polymers. A brief chronological review on the history of high temperature adhesives and laminating resins and the problems associated in working with these materials will be discussed. The processability and mechanical performance of the most popular high temperature adhesives (e.g. FM-34, PPQ, NR056X,

and LARC-13) and laminating resins (e.g. NR-150B2, PMR-15, Thermid 600, and LARC-160) was presented.